J. Fluid Mech. (1977), *vol.* 83, *part* 3, *pp.* 569–604
Printed in Great Britain

Unsteady flow in a supersonic cascade with strong in-passage shocks

By M. E. GOLDSTEIN, WILLIS BRAUN AND J. J. ADAMCZYK

National Aeronautics and Space Administration, Lewis Research Center, Cleveland, Ohio 44135

(Received 12 November 1976)

Linearized theory is used to study the unsteady flow in a supersonic cascade with in-passage shock waves. We use the Wiener–Hopf technique to obtain a closed-form analytical solution for the supersonic region. To obtain a solution for the rotational flow in the subsonic region we must solve an infinite set of linear algebraic equations. The analysis shows that it is possible to correlate quantitatively the oscillatory shock motion with the Kutta condition at the trailing edges of the blades. This feature allows us to account for the effect of shock motion on the stability of the cascade.

Unlike the theory for a completely supersonic flow, the present study predicts the occurrence of supersonic bending flutter. It therefore provides a possible explanation for the bending flutter that has recently been detected in aircraft-engine compressors at higher blade loadings.

1. Introduction

Blade flutter in the fan and compressor stages is one of the most serious problems encountered in the development of modern gas-turbine engines. The major obstacles to predicting this phenomenon, which often occurs when the blades are unstalled and operating supersonically, are primarily fluid mechanical in nature. It is therefore important to understand as well as predict the unsteady supersonic flows in rotating blade rows. The present analysis is directed towards these goals.

As is usually done we represent an incremental annulus of the blade row by a rectilinear two-dimensional cascade. While most modern fans and compressors operate with supersonic flow velocities relative to the blades, the axial velocities entering the blade row are usually subsonic. Under these conditions the leading-edge Mach waves will extend upstream of the cascade and there will be no region of undisturbed flow in front of the blade row (as there is for an isolated airfoil). This is the so-called 'subsonic leading edge locus problem'. Moreover, there will be strong (in the sense that the flow goes from supersonic to subsonic) nearly normal shocks in the blade passage over most of the range of operating conditions. These shocks are clearly detectable in the typical pressure contours for a supersonic fan rotor blade tip shown in figure 1 (Miller & Bailey 1971). Indeed it is this tip region which is known to be most critical from the point of view of blade flutter. It should be noted that, as indicated in the figure, the blade sections have only very small thickness and camber near their tips.

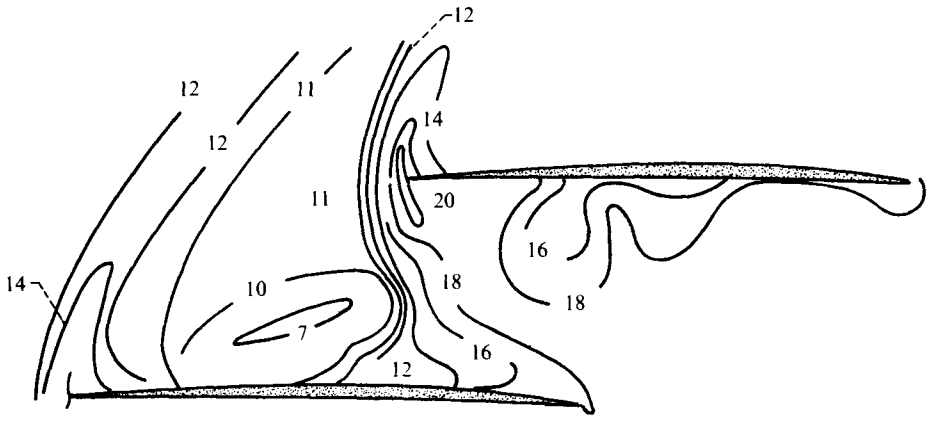

FIGURE 1. Static-pressure contours for rotor at 100% of design speed showing nearly normal in-passage shock. (Close spacing of contours is indicative of rapidly changing pressures.) From Miller & Bailey (1971).

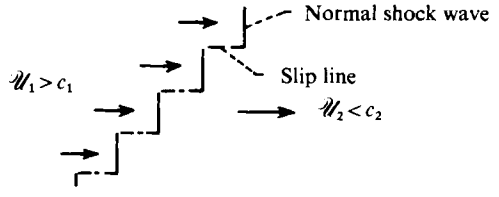

FIGURE 2. Normal-shock configuration.

In order to predict the onset of flutter we allow the blades to undergo a small amplitude harmonic oscillation which superposes a small unsteady motion on an existing inviscid flow field that is steady relative to the blades. Since the blades are thin, it is usual to assume that the steady motion deviates only slightly from a uniform flow. Hence both the steady and the unsteady flow are treated as small perturbations about a uniform 'basic' flow. A number of authors (Nagashima & Whitehead 1974; Kurosaka 1974; Verdon & McCune 1975; Goldstein 1975*a*, *b*; Verdon 1973; Brix & Platzer 1974) have treated the case where the 'basic' flow is entirely supersonic. But since modern fans and compressors can operate at quite high relative tip Mach numbers (1·6 or even higher) the in-passage shock waves are usually strong enough that the mean flow is neither approximately uniform nor entirely supersonic. It is therefore desirable to choose a different 'basic' flow about which to construct the perturbation analysis. This flow must, of course, itself satisfy the inviscid equations of motion. The advantage of using a uniform 'basic' flow is that it leads to equations that can be solves analytically (because they have constant coefficients). However, the 'basic' flow depicted in figure 2 also has this property and still allows us to account for the fact that there are strong shock waves with a moderately high supersonic Mach numbers upstream and relatively low subsonic Mach numbers downstream. In this figure the vertical lines represent the shock waves, across which the flow variables are determined by the Rankine–Hugoniot conditions for normal shocks.†

† In adopting this model we of course neglect the effects of any flow separation that might result from the shock waves.

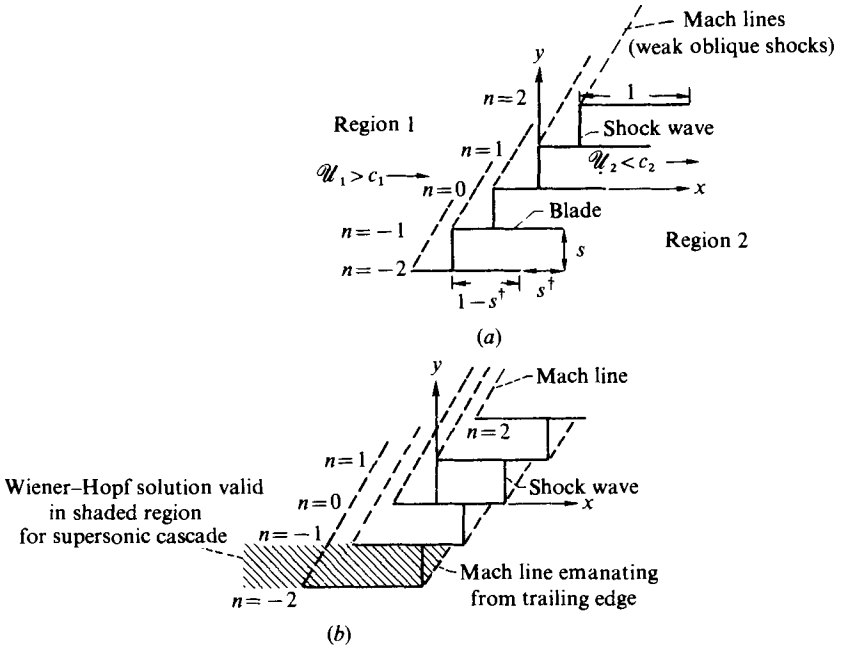

FIGURE 3. Dimensionless cascade configuration. (*a*) Normal shock at leading edge. (*b*) Normal shock at trailing edge.

The present model is somewhat analogous to the one used first by Coupry & Piazzoli (1958) and later by Eckhaus (1959) to predict control-surface buzz on isolated airfoils. However, models of this type clearly provide a much better description of the actual flow in a fan or compressor than they do for an isolated airfoil.

Now, as is well known, the unsteady and steady-state aerodynamics decouple in the linearized approximation, so that the unsteady flow can be calculated independently of the steady flow perturbations. In fact, since the thickness, camber and mean angle of attack of the blades can be shown to influence only the steady flow perturbations, we can calculate the unsteady motion by replacing the blades by a set of zero-thickness flat plates at zero mean incidence such as the ones shown in figure 3.

The fluid is assumed to be an inviscid non-heat-conducting ideal gas with constant specific heats both upstream and downstream of the shock waves. The flow ahead of the shock waves is assumed to be irrotational and isentropic. However, the shock motion can cause the generation of vorticity and entropy gradients in the downstream region.

The problem is formulated in §2, where the governing equations and boundary conditions are deduced. These include an appropriate set of shock conditions to connect the flow in the subsonic and supersonic regions.

Since disturbances cannot propagate upstream in a supersonic flow, it is easy to see from figure 3(*a*) that the motion downstream of the shock cannot influence the upstream region. We take advantage of this fact by replacing the subsonic region by a convenient continuation of the supersonic flow. This allows us to obtain, in §3.1, a closed-form analytical solution for the supersonic region ahead of the shock waves (i.e. we replace the blades by a set of semi-infinite flat plates that extend to infinity

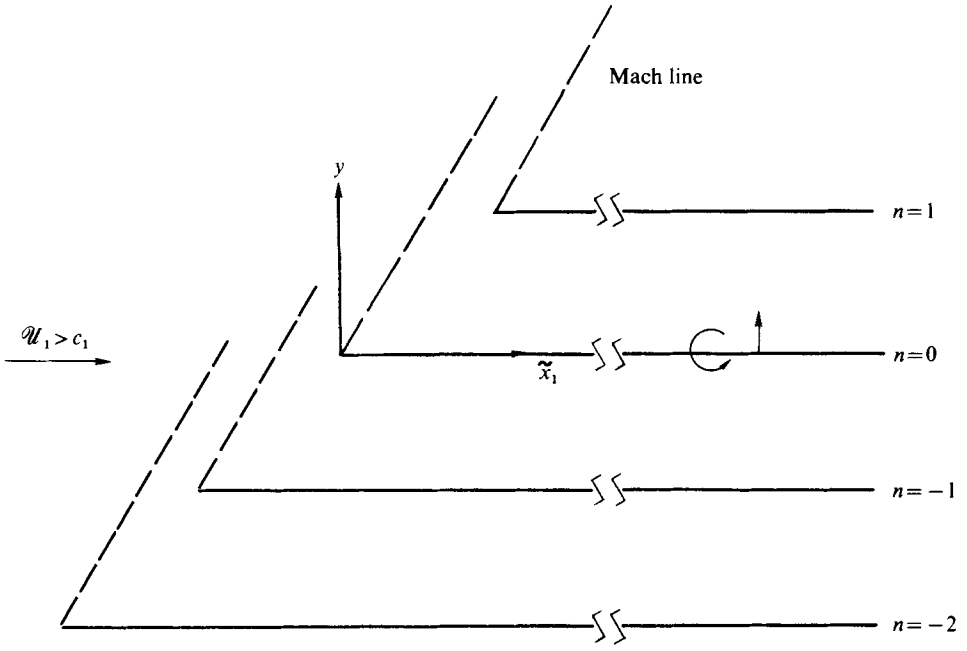

FIGURE 4. Equivalent semi-infinite cascade problem for supersonic region.

downstream (see figure 4) and obtain the solution by the Wiener–Hopf technique). This solution is used in conjunction with the shock jump conditions deduced in §2 to calculate the pressure and axial velocity on the subsonic side of the shock. These quantities, together with those specified on the blade surface, are just sufficient to determine the flow in the subsonic region.

By considering an oscillating cascade of semi-infinite flat plates that extend to infinity in the *upstream* direction, we are able to construct, in §3.2, a solution that satisfies all the boundary conditions in the subsonic region except the ones on the shock waves. This solution has an arbitrarily specified downstream-propagating acoustic field within the cascade. Its composition is determined by requiring that the solution also satisfies the shock boundary conditions. This involves solving an infinite set of algebraic equations for the amplitudes of the incident acoustic waves.

It sometimes happens (especially with precompression blades) that (as indicated in figure 3*b*) the nearly normal shocks appear at the trailing edges rather than at the leading edges of the blades. But since the region upstream of the Mach waves emanating from the trailing edges (see figure 3*b*) would be unaffected by any motion that occurs downstream of these waves if the mean flow were completely supersonic, we can certainly use the semi-infinite flat-plate model illustrated in figure 4 to predict the flow everywhere upstream of normal shocks. Consequently, the procedure described above can also be used to calculate the unsteady flow even when the strong shocks appear at the trailing edges of the blades. We shall, however, consider only the case where the shocks are at the leading edges.

The calculated pressure distributions are discussed in §5.1. The solutions in the subsonic region differ in a number of important respects from those for completely subsonic or completely supersonic flows. This difference is caused by the in-passage

shocks. They affect the surface pressure distributions in the subsonic region by reflecting and transmitting the pressure waves generated by the blade motion. (The pressure waves generated in the downstream region are reflected but not transmitted while the converse is true for those generated upstream.) The impingement of these pressure disturbances also causes changes in shock curvature that result in the emission of downstream-propagating vorticity waves. However, it is shown in §3.2 that these waves produce no real upwash velocity at the blades and therefore have no direct effect on the blade surface forces.

An important consequence of these phenomena is that, unlike the subsonic case, it is possible in the present problem to impose a Kutta condition at the trailing edge without causing the pressure to have a singularity at some other point. In fact, the physical process whereby the flow is able to satisfy the Kutta condition is not the same in the present problem as it is in a subsonic flow but is connected with the shedding of vorticity by the oscillating shock waves and, as indicated in §4.1, the change in circulation caused by the motion of the shock footprints on blades.

In §4.2 the integrated surface forces are used to study the stability of the cascade. It is shown that there is, in addition to the interactions discussed above, another way in which the shock waves can influence the blade forces. The portion of these forces arising from this interaction bears an interesting relation to the circulation about the blades.

Unlike the previous analyses for completely supersonic cascades the present results predict the occurrence of a supersonic bending flutter: a phenomenon which has recently been observed in aircraft-engine fans and compressors. The analysis even correctly predicts the frequency at which this type of flutter occurs.

2. Formulation

We suppose that all lengths are non-dimensionalized by the blade chord c and that the time t is non-dimensionalized with respect to c divided by $\mathscr{U}_1$, the unperturbed velocity of the supersonic stream (measured relative to the blades). The pressure fluctuation p' is non-dimensionalized by ρ_1, the density of the undisturbed supersonic stream, multiplied by $\mathscr{U}_1^2$ and all fluctuating velocities are non-dimensionalized by $\mathscr{U}_1$.

Since the problem is linear, all motion induced by the harmonic oscillations of the blade must also have harmonic time dependence. Upstream of the shock waves this motion is determined by the velocity potential

$$\phi_1(x, y, t) = \Phi_1(x, y)\exp(-i\omega_1 t), \tag{2.1}$$

where $\omega_1 = \omega c/\mathscr{U}_1$ is twice the reduced frequency based on the supersonic velocity and the angular frequency ω of the motion and Φ_1 is governed by the moving-medium reduced wave equation

$$\left(\frac{\partial^2}{\partial y^2} - \beta_1^2\frac{\partial^2}{\partial x^2} + 2iM_1\beta_1^2 k_1\frac{\partial}{\partial x} + \beta_1^4 k_1^2\right)\Phi_1 = 0, \tag{2.2}$$

where $M_1 = \mathscr{U}_1/a_1 > 1$ is the undisturbed free-stream Mach number of the supersonic flow (based on a_1, the undisturbed free-stream speed of sound in this region),

$\beta_1 = (M_1^2-1)^{\frac{1}{2}}$ and $k_1 \equiv \omega_1 M_1/\beta_1^2$. Once the velocity potential's amplitude Φ_1 is known, the amplitudes

$$P_1 = p_1' \exp(i\omega_1 t), \quad V_1 = v_1 \exp(i\omega_1 t), \quad U_1 = u_1 \exp(i\omega_1 t) \tag{2.3}$$

of the pressure fluctuation p_1' and the upwash and axial velocity fluctuations v_1 and u_1, respectively, can be determined from the relations

$$V_1 = \partial\Phi_1/\partial y, \quad U_1 = \partial\Phi_1/\partial x \tag{2.4}$$

and

$$P_1 = (i\omega_1 - \partial/\partial x)\,\Phi_1 \tag{2.5}$$

by differentiation.

The equations governing the flow downstream of the shock waves are obtained by linearizing the inviscid non-heat-conducting continuity and momentum equations about ρ_2, a_2 and $\mathscr{U}_2$, the density, speed of sound and mean flow velocity of the undisturbed subsonic stream relative to the blades (rather than about ρ_1, a_1 and $\mathscr{U}_1$). But since conservation of mass across the steady shock waves requires that ρ_1 and $\mathscr{U}_1$ be related to the corresponding quantities upstream of the shock by $\rho_1\mathscr{U}_1 = \rho_2\mathscr{U}_2$ we can write the non-dimensional linearized equations for the dimensionless subsonic pressure and velocity fluctuations p_2' and $\mathbf{u}_2$ as

$$\left(\frac{\mathscr{U}_1}{\mathscr{U}_2}\frac{\partial}{\partial t}+\frac{\partial}{\partial x}\right)\mathbf{u}_2 = -\nabla p_2', \quad M_2^2\left(\frac{\mathscr{U}_1}{\mathscr{U}_2}\frac{\partial}{\partial t}+\frac{\partial}{\partial x}\right)p_2' = -\nabla.\mathbf{u}_2, \tag{2.6a,b}$$

where $M_2 \equiv \mathscr{U}_2/a_2 < 1$ is the mean steady-flow Mach number downstream of the shock, which (Shapiro 1953, p. 117) is related to M_1 by

$$M_2 = \left[\left(M_1^2+\frac{2}{\mu-1}\right)\Big/\left(\frac{2\mu}{\mu-1}\,M_1^2-1\right)\right], \tag{2.7}$$

where $\mu = c_p/c_v$ is the ratio of specific heats.

Since the downstream flow is vortical, we cannot assume that the velocity and pressure are determined from a single velocity potential in this region. But the splitting theorem (Goldstein 1976, p. 220) guarantees that the velocity can always be decomposed into the sum $\mathbf{u}_2 = \mathbf{u}_2^I + \mathbf{u}_2^S$ of an irrotational ($\nabla\times\mathbf{u}_2^I = 0$) and a solenoidal ($\nabla.\mathbf{u}_2^S = 0$) part in such a way that

$$\left(\frac{\mathscr{U}_1}{\mathscr{U}_2}\frac{\partial}{\partial t}+\frac{\partial}{\partial x}\right)\mathbf{u}_2^S = 0.$$

Then since $\mathbf{u}_2^S$ does not contribute to either of (2.6a,b) the pressure and the part of the velocity represented by $\mathbf{u}_2^I$ can be determined from a velocity potential which satisfies a wave equation in the same fashion as in the irrotational supersonic region while the component $\mathbf{u}_2^S$ can be determined from a stream function. Consequently, there exist a velocity potential $\phi_2(x,y,t) = \Phi_2(x,y)\exp(-i\omega_1 t)$ and a stream function

$$\psi_2(x,y,t) = \Psi_2(x,y)\exp(-i\omega_1 t), \tag{2.8}$$

which determine the amplitudes of the pressure and upwash and axial velocity fluctuations

$$P_2 = p_2' \exp(i\omega_1 t), \quad V_2 = v_2 \exp(i\omega_1 t), \quad U_2 = u_2 \exp(i\omega_1 t) \tag{2.9}$$

by the relations

$$P_2 = \left(i\omega_2 - \frac{\partial}{\partial x}\right)\Phi_2, \quad U_2 = \frac{\partial\Phi_2}{\partial x}+\frac{\partial\Psi_2}{\partial y}, \quad V_2 = \frac{\partial\Phi_2}{\partial y}-\frac{\partial\Psi_2}{\partial x} \tag{2.10}$$

and satisfy the equations

$$\left(\frac{\partial^2}{\partial y^2}+\beta_2^2\frac{\partial^2}{\partial x^2}+2iM_2\beta_2^2k_2\frac{\partial}{\partial x}+\beta_2^4k_2^2\right)\Phi_2=0 \tag{2.11}$$

and

$$(i\omega_2-\partial/\partial x)\Psi_2=0, \tag{2.12}$$

where $\beta_2\equiv(1-M_2^2)^{\frac{1}{2}}$, $k_2=\omega_2M_2/\beta_2^2$ and $\omega_2=\omega c/\mathscr{U}_2$ is the reduced frequency based on the mean velocity $\mathscr{U}_2$ of the subsonic region.

As already indicated, the blades can be replaced by flat plates oscillating harmonically about their mean positions $y=ns$, $(n-1)s^\dagger<x<s^\dagger(n-1)+1$ $(n=0,\ \pm1,\ \pm2,\ \ldots)$ (see figure 3*a*). The unsteady wakes can, to the same order of approximation, be replaced by vortex sheets emanating from the trailing edges of the blades and lying along the lines $y=ns$, $x>s^\dagger(n-1)+1$ $(n=0,\ \pm1,\ \pm2,\ \ldots)$. The mean shock-wave positions are along the line segments $x=ns^\dagger, sn<y<ns+s$ $(n=0,\ \pm1,\ \pm2,\ldots)$. To the order of approximation of the analysis, the boundary conditions on the blades and jump conditions across the shocks and wakes can be transferred to the mean position of these surfaces. Thus since, as shown by Lane (1956), we are required for the purpose of studying flutter to consider only motions in which all blades oscillate harmonically with the same amplitude and a constant but arbitrary interblade phase angle σ, it follows that

$$V(x+ns^\dagger,ns+y)=e^{in\sigma}V(x,y)\quad\text{for}\quad -s^\dagger<x<1-s^\dagger,\quad y=\pm0\quad(n=0,\pm1,\pm2,\ldots), \tag{2.13}$$

where V denotes either V_1 or V_2 depending on which is appropriate for the region of the blade under consideration and $+0$ denotes the limit as $y\to0$ from above while -0 denotes the limit as $y\to0$ through negative values. This equation determines the upwash velocity on the nth blade in terms of that on the zeroth blade while the upwash velocity on the zeroth blade is related to its displacement $W_0\exp(-i\omega_1t)$ by

$$V_2(x,y)=-\frac{\mathscr{U}_2}{\mathscr{U}_1}\left(i\omega_2-\frac{\partial}{\partial x}\right)W_0(x)\quad\text{for}\quad\begin{cases}0<x<1-s^\dagger, & y=+0,\\ -s^\dagger<x<1-s^\dagger, & y=-0,\end{cases} \tag{2.14}$$

$$V_1(x,y)=-\left(i\omega_1-\frac{\partial}{\partial x}\right)W_0(x)\quad\text{for}\quad y=+0,\quad -s^\dagger<x<0. \tag{2.15}$$

The blades can, in general, be undergoing any type of undulation. But in order to simplify the presentation we shall restrict our attention to the case usually considered in turbomachine flutter calculations wherein each incremental blade section is undergoing a rigid-body motion. Then we can write

$$W_0\equiv H_0+A_0(x-d_0), \tag{2.16}$$

where H_0, A_0 and d_0 are constants. H_0 represents the amplitude of a vertical displacement of the point $x=d_0$ while A_0 is the amplitude of the angular displacement about this point.

The pressure and upwash velocity must be continuous across the wake. But in order to satisfy the Kutta condition at the trailing edge we must, in general, allow the axial velocity to be discontinuous.

The flow in the supersonic region is connected to that in the subsonic region by the jump conditions across the shock waves. These conditions are given by equations

(A 2) and (A 3) of appendix A. Hence it follows from (2.3), (2.8), (2.9) and (2.10) that

$$U_2 = -\frac{M_1^2+1}{2M_1^2}P_2 + U_1 + \frac{1}{2}\left[M_1^2+1-\frac{\beta_1^4}{M_1^2}\left(\frac{\mu-1}{\mu+1}\right)\right]P_1, \tag{2.17}$$

$$\frac{\partial P_2}{\partial y} = \left(M_1^2+\frac{\mu-1}{\mu+1}\beta_1^2\right)\frac{\partial P_1}{\partial y} - (\mu+1)\left(\frac{M_1M_2}{\beta_1\beta_2}\right)^2\left(\frac{\partial^2\Psi_2}{\partial y^2}-\omega_2^2\Psi_2\right) \tag{2.18}$$

for $x = ns$, $sn < y < (n+1)s$ $(n = 0, \pm 1, \pm 2, \ldots)$. These equations relate the pressure, axial velocity and vorticity downstream of the shock to the pressure and axial velocity upstream. Finally, we must require that there be only outward-propagating disturbances at large distances from the cascade. Then no disturbance will propagate upstream in the supersonic region ahead of the cascade (relative to the blade-fixed co-ordinates). This completes the specification of the problem.

3. Analytical solution

Before constructing the solution we assume, as is usually done, that there is a small amount of damping in the problem. This amounts to requiring that k_1 and k_2 [which appear in (2.2) and (2.11)] have small positive imaginary parts, say ϵ_1 and ϵ_2. At the end of the problem the damping will be set equal to zero. This allows us to replace the outgoing-wave boundary conditions at infinity by conditions of boundedness.

The boundary condition (2.13) requires that the solution possess a certain blade-to-blade periodicity but we shall require it to satisfy the stronger periodicity condition

$$\Theta(x+ns^\dagger, ns+y) = e^{in\sigma}\Theta(x,y), \tag{3.1}$$

where Θ can denote any of the physical variables V_1, V_2, P_1, P_2, etc. Once it has been shown that such a solution can be made to satisfy all the boundary conditions in the problem, the *Ansatz* will be justified.

Since disturbances cannot propagate upstream in a supersonic flow, it is easy to see from figure 3 that the fluid in region 1 cannot be affected by anything that happens at or behind the shock waves. Hence we can determine the solution in this region independently of the one in region 2. Then, once this solution has been found, the pressure and axial velocity downstream of the shock wave can be obtained from (2.17) and (2.18). These quantities together with the remaining boundary conditions are just sufficient to determine the flow everywhere in region 2.

3.1. *Solution in supersonic region*

We first determine the solution in the supersonic region. To this end we notice that, since the flow in this region is uninfluenced by anything that happens downstream of the shock waves, the problem can be replaced by the equivalent problem of an oscillating cascade of semi-infinite blades in a completely supersonic flow. The configuration is illustrated in figure 4. The reason for doing this is that the new problem can be solved explicitly by using the Wiener–Hopf technique. In fact Carlson & Heins (1947) carried out an analogous calculation for the scattering of electromagnetic waves while Mani & Horvay (1970) calculated the reflexion of an acoustic wave by a semi-infinite cascade in a subsonic flow. (Although the present analysis is formally similar to these previous studies, differences in the choice of branch cuts and integration

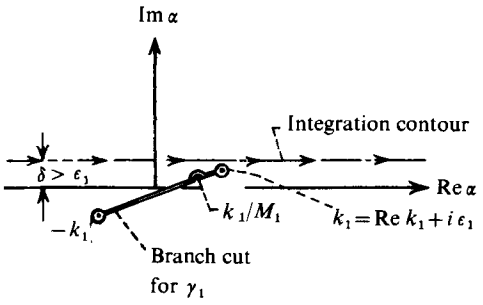

FIGURE 5. Integration contour and branch cut in complex α plane.

contours cause marked differences in the subtler aspects of the solution that must be treated in ways that are by no means straightforward.)

The function Φ_1 of (2.2) is essentially the sum of the disturbance fields due to the individual blades. We therefore attempt to represent it as a superposition

$$\Phi_1 = \sum_{n=-\infty}^{\infty} \Phi_1^{(n)} \tag{3.2}$$

of the contributions from the individual blades. Then since (2.2) possesses a separation-of-variables solution $\exp\{-i[(\alpha - M_1 k_1)x - \beta_1 \gamma_1 y]\}$, where $\gamma_1 \equiv (\alpha^2 - k_1^2)^{\frac{1}{2}}$, it is reasonable to express $\Phi_1^{(n)}$ as the Fourier integral

$$\Phi_1^{(n)} = \frac{\operatorname{sgn} y_n}{2\pi} \int_{-\infty+i\delta}^{\infty+i\delta} f_{(n)}^1(\alpha) \exp\{-i(\alpha - M_1 k_1)s^\dagger\} \exp\{-i[(\alpha - M_1 k_1)x_n - \beta_1 \gamma_1 |y_n|]\} d\alpha, \tag{3.3}$$

where we have put $x_n = x - ns^\dagger$ and $y_n = y - ns$ $(n = 0, \pm 1, \pm 2, \ldots)$ and in order to ensure that no waves propagate upstream and that the solution remain bounded at infinity (i.e. only outward-propagating waves exist) we have chosen the integration contour in the complex α plane and the branch cut for the square root γ_1 in the manner indicated in figure 5. The height δ of this contour above the real axis is assumed to be a quantity of the order of the damping ϵ_1 but otherwise is as yet unspecified.

The signum function is defined as usual by $\operatorname{sgn} y = \pm 1$ for $y \gtrless 0$ and its insertion causes Φ_1 to have the jump discontinuity

$$\begin{aligned}[\Phi_1(x)]_n &\equiv \lim_{\epsilon \to 0} [\Phi_1(x, ns+\epsilon) - \Phi_1(x, ns-\epsilon)] = [\Phi_1^{(n)}(x)]_n \\ &= \frac{1}{\pi} \int_{-\infty+i\delta}^{\infty+i\delta} f_n^{(1)}(\alpha) \exp\{i(M_1 k_1 - \alpha) x_{(n-1)}\} d\alpha \end{aligned} \tag{3.4}$$

across the line $y = ns$ passing through the nth blade. The introduction of this discontinuity will cause the upwash velocity $V_1 = \partial \Phi_1 / \partial y$ to be continuous everywhere.

Now it is easy to verify that the solution (3.2) will satisfy the periodicity condition (3.1) if we take

$$f_n^{(1)}(\alpha) = e^{in\sigma} f_0^{(1)}(\alpha) \quad \text{for} \quad n = 0, \pm 1, \pm 2, \ldots. \tag{3.5}$$

Inserting this into (3.3) and using the result in (3.2) shows that

$$\Phi_1 = \frac{1}{2\pi} \int_{-\infty+i\delta}^{\infty+i\delta} f_0^{(1)}(\alpha) \Lambda_1(\alpha, y) \exp\{-i(\alpha - M_1 k_1)\tilde{x}_1\} d\alpha, \tag{3.6}$$

where we have put $\tilde{x}_1 \equiv x + s^\dagger$ and

$$\Lambda_1(\alpha, y) = \sum_{n=-\infty}^{\infty} (\operatorname{sgn} y_n) \exp\{i[n(\sigma + s^\dagger \alpha - s^\dagger M_1 k_1) + \beta_1 \gamma_1 |y_n|]\}. \tag{3.7}$$

We now set $\delta = M_1 \epsilon_1$. Then since $\operatorname{Im}(\alpha - M_1 k_1) = 0$ and $\operatorname{Im} \gamma_1 > 0$ for $\delta = M_1 \epsilon_1$, $-\infty < \operatorname{Re} \alpha < \infty$, it follows that $|\exp\{i[(\alpha - M_1 k_1) n s^\dagger + \beta_1 \gamma_1 |y_n|]\}| < 1$ everywhere on the contour of integration in (3.6). We can therefore use the geometric series

$$\sum_{n=0}^{\infty} Z^n = (1 - Z)^{-1} \quad \text{for} \quad |Z| < 1$$

to sum the series in (3.7) and thereby obtain

$$\Lambda_1(\alpha, y) = \frac{1}{2i}\left[\frac{\exp\{i(\Delta_1^- + \beta_1 \gamma_1 y)\}}{\sin \Delta_1^-} + \frac{\exp\{i(\Delta_1^+ - \beta_1 \gamma_1 y)\}}{\sin \Delta_1^+}\right] \quad \text{for} \quad 0 \leqslant y \leqslant s, \tag{3.8}$$

where $\Delta_1^\mp \equiv \frac{1}{2}(\sigma - M_1 k_1 s^\dagger + \alpha s^\dagger \pm \beta_1 \gamma_1 s)$.

The upwash velocity can now be written as

$$V_1(x, y) = \frac{\partial \Phi_1}{\partial y} = \frac{1}{2\pi} \int_{-\infty + i\epsilon_1 M_1}^{\infty + i\epsilon_1 M_1} f_0^{(1)}(\alpha) \kappa_1(\alpha, y) \exp\{-i(\alpha - M_1 k_1)\tilde{x}_1\} d\alpha, \tag{3.9}$$

where

$$\kappa_1(\alpha, y) \equiv \partial \Lambda_1(\alpha, y)/\partial y. \tag{3.10}$$

Equations (3.7) and (3.10) show that this quantity is indeed continuous everywhere. However, we must also require that the remaining physical quantities be continuous along the lines $y = ns$, $-\infty < x < (n-1)s^\dagger$ $(n = 0, \pm 1, \pm 2, \ldots)$ that extend forward of the leading edges of the blades. This will occur if Φ_1 is continuous across these lines. Moreover, the fact that Φ_1 satisfies the periodicity condition (3.1) ensures that it will be continuous across all of these lines if it is continuous across the line $y = 0$, $-\infty < x < -s^\dagger$ passing through the $n = 0$ blade. It follows from (3.4) and (3.5) that this will occur if

$$\frac{1}{2\pi} \int_{-\infty + i\epsilon_1 M_1}^{\infty + i\epsilon_1 M_1} f_0^{(1)}(\alpha) \exp\{-i(\alpha - M_1 k_1)\tilde{x}_1\} d\alpha = 0 \quad \text{for} \quad \tilde{x}_1 < 0. \tag{3.11}$$

The solution now satisfies all the boundary conditions except those imposed on the upwash at the blade surface. The fact that V_1 satisfies condition (3.1) again ensures that (2.13) will be satisfied. Hence it is only necessary to require that (2.15) be satisfied. And since we are at liberty to choose the upwash velocity on the line segment $y = 0$, $x > 0$ arbitrarily, we find from (3.9) that

$$\frac{1}{2\pi} \int_{-\infty + i\epsilon_1 M_1}^{\infty + i\epsilon_1 M_1} f_0^{(1)}(\alpha) \kappa_1(\alpha, 0) \exp\{-i(\alpha - M_1 k_1)\tilde{x}_1\} \times d\alpha = \left(-i\omega_1 + \frac{\partial}{\partial x}\right) W_0(x) \quad \text{for} \quad \tilde{x}_1 > 0. \tag{3.12}$$

Thus if we can determine the function $f_0^{(1)}(\alpha)$ that satisfies these two equations we shall have succeeded in constructing the proper solution for region 1.

Equations (3.11) and (3.12) constitute a set of dual integral equations which can be solved for $f_0^{(1)}(\alpha)$ by the Wiener–Hopf technique. The procedure is outlined in

appendix B. The result is given by equation (B 10). When this is substituted into (3.6) we obtain

$$\Phi_1 = \frac{1}{2\pi}\int_{-\infty+i\epsilon_1 M_1}^{\infty+i\epsilon_1 M_1} \exp\{-i(\alpha - M_1 k_1)(x+s^\dagger)\}\,\frac{\kappa_1^-(M_1 k_1 - i\epsilon_0)}{\kappa_1^+(\alpha)}\,\frac{\Lambda_1(\alpha, y)}{(\alpha - M_1 k_1 + i\epsilon_0)} \times \left(D_-^{(1)} + \frac{i\omega_1 A_0}{\alpha - M_1 k_1 + i\epsilon_0}\right) d\alpha, \quad (3.13)$$

where

$$D_-^{(1)} = iA_0\left\{1 + \omega_1 \frac{[\kappa_1^-(M_1 k_1 - i\epsilon_0)]'}{\kappa_1^-(M_1 k_1 - i\epsilon_0)}\right\} + \omega_1[H_0 - A_0(s^\dagger + d_0)],$$

ϵ_0 is a small positive number which can be put equal to zero after the contour integral has been evaluated and $\kappa_1^{\mp}(\alpha)$ are non-zero analytic functions that have algebraic behaviour at infinity in the upper/lower half-planes and are determined by the functional equation (B 4). The latter quantities are calculated in appendix C [κ_1^- is given by (C 5)–(C 7) and κ_1^+ can then be determined from (B 4) and (C 1)].

This completes the solution to the problem in region 1. The pressure and velocity can be determined at any point of region 1 by substituting (3.13) into (2.4) and (2.5) and carrying out the indicated differentiations.

We need to know the pressure $P_1(0, y)$ and axial velocity $U_1(0, y)$ (for $0 < y < s$) on the supersonic side of the shock in order to obtain the solution in the subsonic region. Since these quantities are calculated by differentiating (3.13) with respect to x their integrands will contain the function $\Lambda_1(\alpha, y)/\kappa_1^+(\alpha) = \Lambda_1(\alpha, y)/[\kappa_1(\alpha, 0)\kappa_1^-(\alpha)]$, and since this function depends on γ_1 we might anticipate that it will have the same branch-cut singularity as γ_1. But in appendix C we show that no such singularities can occur. The same arguments can be used to show that the singularities of $\Lambda_1(\alpha, y)$ are at most poles. Hence we can conclude that the singularities of the integrands in the equations for P_1 and U_1 are also at most poles. The residue theorem can therefore be used to evaluate the integrals. Since $x = 0$ and $y < s$ on the surface of the shock and $s^\dagger > \beta_1 s$ for subsonic axial velocity, it is easy to show that the integrands will vanish exponentially fast as $\alpha \to \infty$ in the lower half-plane and become unbounded as $\alpha \to \infty$ in the upper half-plane. Hence we must complete the contour with a large semicircle in the lower half-plane. The value of the integrals will then be equal to $-2\pi i$ times the sum of the residues at their poles in the lower half α plane. These poles occur at the infinite set of points $\lambda_n^{(1)}$ ($n = 0, \pm 1, \pm 2, \ldots$) defined in (C 2) and at the point $\alpha = M_1 k_1 - i\epsilon_0$. After the contour integrals have been evaluated we can put $\epsilon_1 = \epsilon_0 = 0$. When these operations have been carried out we find that the pressure and axial velocity just upstream of the shock are given by

$$U_1(0, y) = \sum_{n=0}^{\infty} Q_n \cos\frac{n\pi y}{s} + iA_0\omega_1 f_1(y; M_1\omega_1), \quad 0 < y < s, \quad (3.14)$$

$$P_1(0, y) = \sum_{n=0}^{\infty} R_n \cos\frac{n\pi y}{s} - \omega_1[(H_0 - d_0 A_0)\omega_1 + 2iA_0] f_1(y; M_1\omega_1) - i\omega_1^2 A_0\left[f_2(y; M_1\omega_1) + \frac{\partial}{\partial\omega_1} f_1(y; M_1\omega_1)\right], \quad 0 < y < s, \quad (3.15)$$

where

$$Q_n = Q_n^+ + Q_n^-, \quad R_n = R_n^+ + R_n^-, \quad (3.16)$$

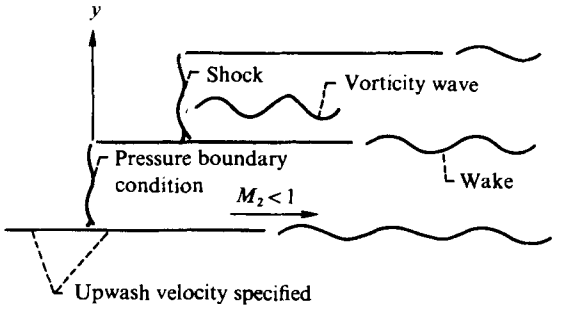

FIGURE 6. Boundary-value problem in subsonic region.

$$Q_n^{\pm} = \frac{e^{i(\sigma - n\pi)} - \exp\{i(M_1 k_1 \mp \lambda_n^{(1)}) s^{\dagger}\}}{\pm \lambda_n^{(1)} s \beta_1^2 (1 + \delta_{n,0})} \frac{\kappa_1^-(M_1 k_1)}{\kappa_1^-(\pm \lambda_n^{(1)})} \left(D_-^{(1)} + \frac{i\omega_1 A_0}{\pm \lambda_n^{(1)} - M_1 k_1} \right), \tag{3.17}$$

$$R_n^{\pm} = -\frac{-(k_1/M_1) \pm \lambda_n^{(1)}}{\pm \lambda_n^{(1)} - M_1 k_1} Q_n^{\pm}, \quad \lambda_n^{(1)} = [k_1^2 + (n\pi/\beta_1 s)^2]^{\frac{1}{2}}, \tag{3.18}$$

$$f_1(y;\omega) \equiv \frac{e^{i\sigma} \cos \omega y - \cos \omega(s-y)}{\omega \sin \omega s}, \quad f_2(y;\omega) \equiv \frac{is^{\dagger} e^{i\sigma} \cos \omega y}{\omega \sin \omega s}. \tag{3.19}$$

By using the asymptotic representation (C 8) for κ_1^- it is easy to show that $Q_n = O(n^{-2})$ and $R_n = O(n^{-2})$ as $n \to \infty$. Hence the infinite series in (3.14) and (3.15) are absolutely convergent and as a result represent continuous functions.

The pressure $P_1(x, 0+)$ on the portion $-s^{\dagger} < x < 0$ of the airfoil surface is evaluated in appendix D. We are now ready to calculate the solution in the subsonic region.

3.2. *Solution in subsonic region*

The boundaries of region 2 are sketched in figure 6. The pressure and axial velocity are specified on the shocks by (2.17), (2.18) and (3.14)–(3.19) while the upwash velocity on the blade surfaces is given by (2.13), (2.14) and (2.16). We must also require that the pressure and upwash velocity be continuous across the wakes and that only outward-propagating disturbances exist far downstream. Finally we make the solution unique by requiring that it satisfies a Kutta condition at the trailing edges of the blades.

Equation (2.12) can be integrated immediately to obtain

$$\begin{aligned}\Psi_2(x,y) &= \Omega(y) \exp(i\omega_2 x) \\ &= \left\{\Omega(y) - \frac{\Omega(s(n+1)) \sinh \omega_2(y - ns) + \Omega(ns) \sinh \omega_2[s(n+1) - y]}{\sinh \omega_2 s}\right\} \exp(i\omega_2 x) \\ &\quad + \frac{\Omega(s(n+1)) \sinh \omega_2(y - ns) + \Omega(ns) \sinh \omega_2[s(n+1) - y]}{\sinh \omega_2 s} \exp(i\omega_2 x) \\ &\qquad \text{for} \quad ns < y < (n+1)s \quad (n = 0, \pm 1, \pm 2, \ldots),\end{aligned} \tag{3.20}$$

where $\Omega(y)$ is an as yet arbitrary function of y. Notice that Ψ_2 will satisfy the periodicity condition (3.1) only if we require that

$$\Omega(y + ns) = \exp\{in(\sigma - \omega_2 s^{\dagger})\} \Omega(y) \quad \text{for} \quad 0 < y < s \quad (n = 0, \pm 1, \pm 2, \ldots).$$

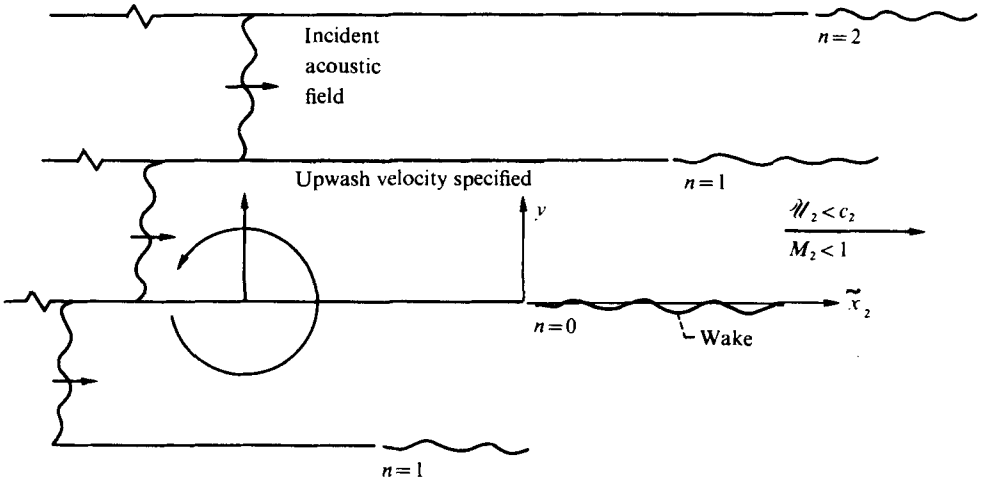

FIGURE 7. Equivalent problem for subsonic cascade.

Then it is easy to see from (2.10) that the (reduced) velocity potential

$$\frac{\Omega(s(n+1))\cosh\omega_2(y-ns)-\Omega(ns)\cosh\omega_2[s(n+1)-y]}{i\sinh\omega_2 s}\exp(i\omega_2 x)$$

will satisfy the wave equation (2.11) and the periocity condition (3.1) (and have outgoing-wave behaviour at downstream infinity) while producing the same velocity and pressure fields as the second term in (3.20). Hence we can always suppose that the effect of that term has been incorporated into Φ_2 and, consequently, that Ψ'_2 is given by the first term in (3.20). But this quantity is identically zero along the lines $y = ns$ ($n = 0, \pm 1, \pm 2, \ldots$). Hence it follows from (2.10) that the vortical solution (which is determined by Ψ'_2) has zero upwash velocity on the blades, has no jump in pressure or upwash velocity across the wakes, and in fact makes no contribution to the pressure field at any point of the flow. It therefore follows from (2.14) and (2.15) that it will neither contribute to the boundary conditions on the blades nor the jump conditions across the wakes and consequently that these conditions must be satisfied entirely by the acoustic portion of the solution (which is determined by Φ_2).

We can construct a solution to the wave equation (2.11) that will satisfy the upwash boundary condition given by (2.13), (2.14) and (2.16), the correct jump conditions across the wake and the radiation condition at downstream infinity and still retain enough arbitrariness to satisfy the remaining boundary condition on the shock waves by considering the cascade of semi-infinite flat plates shown in figure 7. The plates now extend to infinity in the upstream direction and the mean flow is assumed to be uniform at the downstream subsonic Mach number M_2.

The desired solution is a composite of the outgoing-wave solution $\Phi_2^{(2)}$ that satisfies the upwash boundary conditions (2.13), (2.14) and (2.16) everywhere on the plates (together with the correct wake jump conditions and trailing-edge Kutta condition) and a solution $\Phi_2^{(1)}$ that has zero upwash velocity on the plates but has an arbitrarily specified downstream-propagating wave field far upstream from the trailing edge. We of course require that the latter solution also satisfies the Kutta condition, the wake jump condition and the radiation condition at downstream infinity and that its

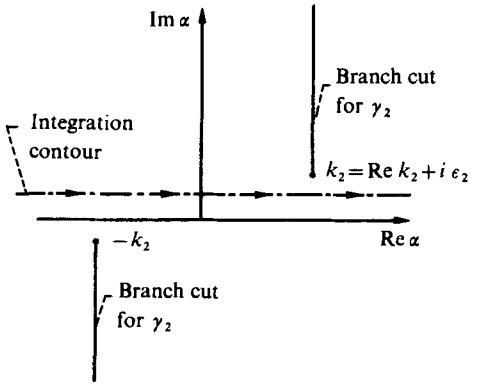

FIGURE 8. Integration contour and branch cut in complex α plane.

upstream incident wave field satisfies the periodicity condition (3.1). The composite solution clearly satisfies all the conditions imposed on the subsonic potential except the ones on the shock waves. But we shall show subsequently that the upstream wave field can be so adjusted that these conditions are also satisfied.

The second portion $\Phi_2^{(1)}$ of the composite solution has, in effect, already been found by Mani & Horvay (1970). Their results imply

$$\Phi_2^{(1)} = \frac{1}{i}\sum_{n=0}^{\infty} B_n \left\{ \frac{\exp(i\eta_n^+ x)}{k_2/M_2 - \lambda_n^{(2)}} \cos\frac{n\pi y}{s} - \frac{\exp(i\eta_n^+)}{4\pi i}\,[e^{i(n\pi-\sigma)} - \exp(-i\eta_n^+ s^\dagger)] \right.$$
$$\left. \times \int_{-\infty+i\delta_2}^{\infty+i\delta_2} \frac{\kappa_2^-(-\lambda_n^{(2)})}{\kappa_2^-(\alpha)} \frac{\Lambda_2(\alpha,y)\exp\{-i(\alpha+M_2k_2)\tilde{x}_2\}}{[\alpha+\lambda_n^{(2)}](\alpha+k_2/M_2)}\,d\alpha \right\} \quad \text{for} \quad 0<y<s, \tag{3.21}$$

where $\tilde{x}_2 = x + s^\dagger - 1$,

$$\Lambda_2(\alpha,y) = \frac{1}{2i}\left(\frac{\exp(-\beta_2\gamma_2 y + i\Delta_2^+)}{\sin\Delta_2^+} + \frac{\exp(\beta_2\gamma_2 y + i\Delta_2^-)}{\sin\Delta_2^-}\right) \quad \text{for} \quad 0<y<s, \tag{3.22}$$

$$\Delta_2^\pm \equiv \tfrac{1}{2}(\sigma + M_2k_2s^\dagger + \alpha s^\dagger) \pm s\beta_2\gamma_2/2i, \tag{3.23}$$

$$\eta_n^\pm \equiv -M_2k_2 \pm \lambda_n^{(2)}, \tag{3.24}$$

$$\lambda_n^{(2)} \equiv i[(n\pi/s\beta_2)^2 - k_2^2]^{\frac{1}{2}}, \tag{3.25}$$

$-\epsilon_2 < \delta_2 < \epsilon_2 \equiv \operatorname{Im} k_2$ and $\gamma_2 \equiv (\alpha^2 - k_2^2)^{\frac{1}{2}}$ with the branch of the square roots chosen in the manner indicated in figure 8. The B_n are the amplitudes of the incident infinite-duct waves $[\exp(i\eta_n^+ x)]\cos(n\pi y/s)$ and are, at this point, arbitrary. Finally, the function $\kappa_2^-(\alpha)$ is analytic in the lower half-plane with algebraic behaviour at infinity and arises from the factorization

$$\kappa_2^-(\alpha)/\kappa_2^+(\alpha) = -\frac{\partial\Lambda_2(\alpha,y)}{\partial y}\bigg|_{y=0} \Big/ \left(\alpha + \frac{k_2}{M_2}\right) \quad \text{for} \quad \operatorname{Im}\alpha = \delta_2, \quad -\infty < \operatorname{Re}\alpha < \infty \tag{3.26}$$

of the kernel function $-(\partial\Lambda_2(\alpha,y)/\partial y)_{y=0}/(\alpha + k_2/M_2)$ in the same way that κ_1^- arose in the supersonic problem of §3.1. It is given in infinite-product form by equation (E 1). When $x < 1 - s^\dagger$ the second term in the summand of (3.21) merely represents the reflected waves produced by the impingement of the incident wave

$$[\exp i\eta_n^+ x]\cos(n\pi y/s)$$

on the open end of the cascade. In fact, as we shall see below, it can be expressed entirely in terms of the upstream-propagating waves $[\exp i\eta_n^- x]\cos(n\pi y/s)$.

The portion $\Phi_2^{(2)}$ of Φ_2 can be obtained by a procedure that is in its general aspects the same as that used to obtain the supersonic solution and in its detailed aspects similar to the Mani–Horvay (1970) procedure that was used to obtain $\Phi_2^{(1)}$. We therefore again give only the final result, which can be written as

$$\Phi_2^{(2)} = \frac{1}{2\pi}\int_{-\infty+i\delta_1}^{\infty+i\delta_1} \frac{\Lambda_2(\alpha,y)\kappa_2^+(-M_2k_2+i\epsilon_0)}{(\alpha+k_2/M_2)\kappa_2^-(\alpha)(\alpha+M_2k_2-i\epsilon_0)}\exp\{-i(\alpha+M_2k_2)\tilde{x}_2\} \times\left(D_+^{(2)}+\frac{i\omega_1A_0}{\alpha+M_2k_2-i\epsilon_0}\right)d\alpha, \tag{3.27}$$

where

$$D_+^{(2)} = \omega_1[H_0+A_0(1-s^\dagger-d_0)]+iA_0\left\{\frac{\omega_1}{\omega_2}+\omega_1\frac{[\kappa_2^+(-M_2k_2+i\epsilon_0)]'}{\kappa_2^+(-M_2k_2+i\epsilon_0)}\right\},$$

κ_2^+ is given by equation (E 5) and, as before, $\epsilon_0 > M_2\epsilon_2$ is a small positive constant that can be put equal to zero after the contour integrals have been evaluated. This result should be compared with equation (3.13) for the supersonic region.

We must now prove that we can adjust the function Ω in (3.20) and the constants B_n in (3.21) to make

$$\Phi_2(x,y) = \Phi_2^{(1)}(x,y)+\Phi_2^{(2)}(x,y) \tag{3.28}$$

and Ψ_2 satisfy the boundary conditions (2.17) and (2.18). But since, as in the supersonic case, the singularities of the integrand in (3.21) are all poles, we can use the residue theorem to evaluate the integral. For $x_2 < 0$ the contour must be closed in the upper half-plane, so that inserting (3.26) and (3.22) into (3.21) and applying the residue theorem yields

$$\Phi_2^{(1)} = \frac{1}{i}\sum_{n=0}^{\infty}\left[\frac{B_n\exp(i\eta_n^+x)}{(k_2/M_2)-\lambda_n^{(2)}}+\left(\sum_{m=0}^{\infty}B_mK_{m,n}\right)\frac{\exp(i\eta_n^-\tilde{x}_2)}{\lambda_n^{(2)}+(k_2/M_2)}\right]\cos\frac{n\pi y}{s} \quad \text{for} \quad \tilde{x}_2<0, \quad 0<y<s, \tag{3.29}$$

where

$$K_{m,n} = \frac{\exp(i\eta_m^+)}{2(1+\delta_{n,0})}[\exp\{i(m\pi-\sigma)\}-\exp(-i\eta_m^+s^\dagger)][\exp\{i(\sigma-\eta_n^-s^\dagger+n\pi)\}-1] \times\frac{\kappa_2^-(-\lambda_m^{(2)})(\lambda_n^{(2)}+(k_2/M_2))}{\kappa_2^+(\lambda_n^{(2)})(\lambda_n^{(2)}+\lambda_m^{(2)})s\beta_2^2\lambda_n^{(2)}}.$$

On the other hand, since we can require that Ψ_2 vanishes at $y = 0$ and s, $\Omega(y)$ can be expanded in an absolutely convergent sine series to obtain

$$\Psi_2 = \sum_{n=1}^{\infty}b_n\sin\left(\frac{n\pi y}{s}\right)\exp(i\omega_2x) \quad \text{for} \quad 0\leqslant y\leqslant s. \tag{3.30}$$

It is now clear that substituting this equation together with (3.28) and (3.29) into (2.10) and inserting the results in the boundary conditions (2.17) and (2.18) we obtain expressions which have the form of Fourier sine and cosine series with unknown coefficients (which are the B_n and b_n) equated to known functions of y. Then since the sines and cosines both form a complete set on the interval $(0, s)$, this shows that

(3.27)–(3.30) can be made to satisfy (2.17) and (2.18). In fact, we can evaluate the contour integral in (3.27) as was done above to obtain

$$P_2^{(2)} \equiv \left(i\omega_2 - \frac{\partial}{\partial x}\right)\Phi_2^{(2)} = \sum_{n=0}^{\infty} H_n \exp(i\eta_n^- \tilde{x}_2)\cos\left(\frac{n\pi y}{s}\right) - \omega_1\{H_0 + A_0(x-d_0)]\omega_2 + 2iA_0\}f_1(y, M_2\omega_2) - i\omega_1\omega_2 A_0\left[f_2(y, M_2\omega_2) + \frac{\partial}{\partial\omega_2}f_1(y, M_2\omega_2)\right], \quad (3.31)$$

$$U_2^{(2)} = \frac{\partial\Phi_2^{(2)}}{\partial x} = -\sum_{n=0}^{\infty}\frac{\lambda_n^{(2)} + M_2 k_2}{\lambda_n^{(2)} + (k_2/M_2)} H_n \exp(i\eta_n^- \tilde{x}_2)\cos\left(\frac{n\pi y}{s}\right) + iA_0\omega_1 f_1(y, M_2\omega_2),$$

where

$$H_n \equiv \frac{\exp\{i(\sigma - \eta_n^- s^\dagger + n\pi)\} - 1}{s\beta_2^2(1+\delta_{n,0})\lambda_n^{(2)}}\left[\frac{\kappa_2^+(-M_2k_2)(\lambda_n^{(2)} + (k_2/M_2))}{\kappa_2^+(\lambda_n^{(2)})(\lambda_n^{(2)} + M_2k_2)}\right]\left(D_+^{(2)} + \frac{i\omega_1 A_0}{\lambda_n^{(2)} + M_2k_2}\right)$$

and f_1 and f_2 are given by (3.19). Then since

$$P_2 = (i\omega_2 - \partial/\partial x)\Phi_2^{(1)} + P_2^{(2)} \quad (3.32)$$

and

$$U_2 = \partial\Phi_2^{(1)}/\partial x + U_2^{(2)} + \partial\Psi_2/\partial y,$$

inserting these results together with (3.14) and (3.15) into the boundary conditions (2.17) and (2.18), exploiting the orthogonality of the sines and cosines on $(0, s)$ and finally eliminating the b_n from the result we obtain

$$-\frac{2}{s}\frac{F_n}{1+\delta_{n,0}} = B_n a_n^+ + a_n^- \exp\{-i\eta_n^-(1-s^\dagger)\}\sum_{m=0}^{\infty} B_m K_{m,n}, \quad (3.33)$$

where $a_n^\pm \equiv [\lambda_n^{(2)}]^2 \pm 2M_2k_2\lambda_n^{(2)} + (k_2/M_1)^2$ and the inhomogeneous term F_n is given in appendix F.

4. Discussion and results

4.1. *Surface pressure distributions*

Once (3.33) has been solved for the B_n, (3.29), (3.31) and (3.32) can be used to calculate the pressure on the subsonic portion of the upper surface of the $n = 0$ blade and, in view of (3.1), on the portion of the lower surface lying between $x = -s^\dagger$ and $x = 1 - 2s^\dagger$. Equations (G 1) and (G 2) can be used to calculate the pressure on the remainder of the lower surface.

Since the second term in (3.29) represents the upstream-propagating waves resulting from the reflexion of the incident acoustic field $B_n \exp(i\eta_n^+ x)\cos(n\pi y/s)$ by the back end of the cascade, the infinite sum in (3.33) must represent the effect of these reflexions in that equation. But since (except perhaps at the in-passage duct resonance condition) most of these reflected waves will be evanescent and since evanescent waves usually decay quite rapidly in a duct, there should be at most one or two terms that contribute significantly to the sum in (3.33). In fact, the summation can often be neglected entirely, in which case (3.33) will yield an explicit solution for the B_n.

The calculated surface pressure amplitudes (non-dimensionalized by $\rho_1 \mathscr{U}_1^2 A_0$) are shown in figures 9–14. For simplicity we present only results for a single cascade configuration undergoing a pure torsional oscillation about the centre of the blade. The stagger angle is 60° and the solidity is 1·3 for this cascade. But even with these conditions fixed, the pressure distributions depend on a number of parameters and

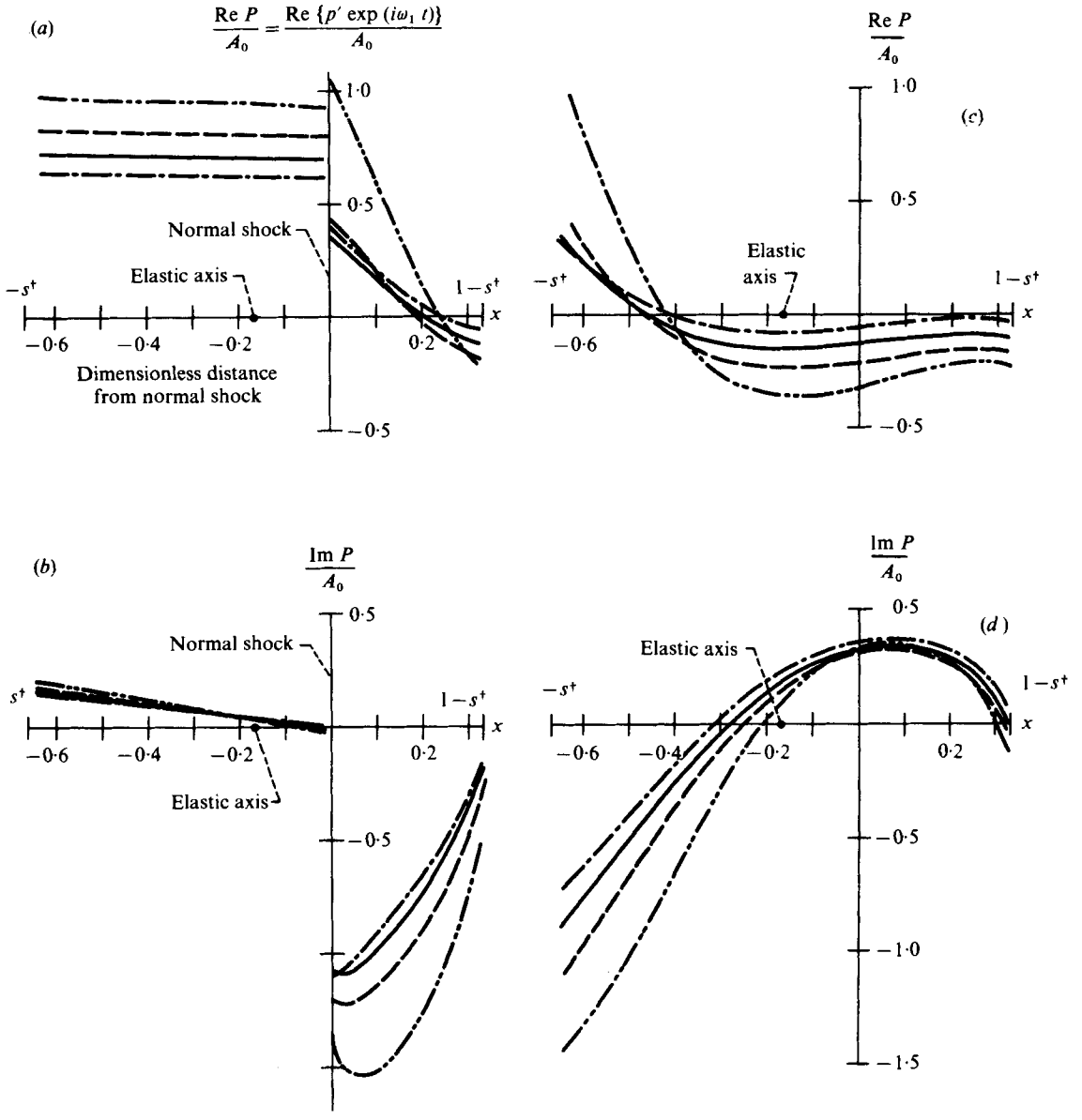

FIGURE 9. Non-dimensionalized surface pressure amplitudes acting on a cascade undergoing a pure pitching oscillation about the centre of the blades. Stagger angle = 60°; solidity = 1·3; interblade phase angle $\sigma = 0$; reduced frequency $\frac{1}{2}\omega_1 = 0{\cdot}25$. (*a*) In-phase component (real part) of dimensionless pressure amplitude acting on upper surface. (*b*) Out-of-phase component (imaginary part) of dimensionless pressure amplitude acting on upper surface. (*c*) In-phase component (real part) of dimensionless pressure amplitude acting on lower surface. (*d*) Out-of-phase component (imaginary part) of dimensionless pressure amplitude acting on lower surface. -·--, $M_1 = 1{\cdot}2$; ---, $M_1 = 1{\cdot}4$; ——, $M_1 = 1{\cdot}6$; -··-, $M_1 = 1{\cdot}8$.

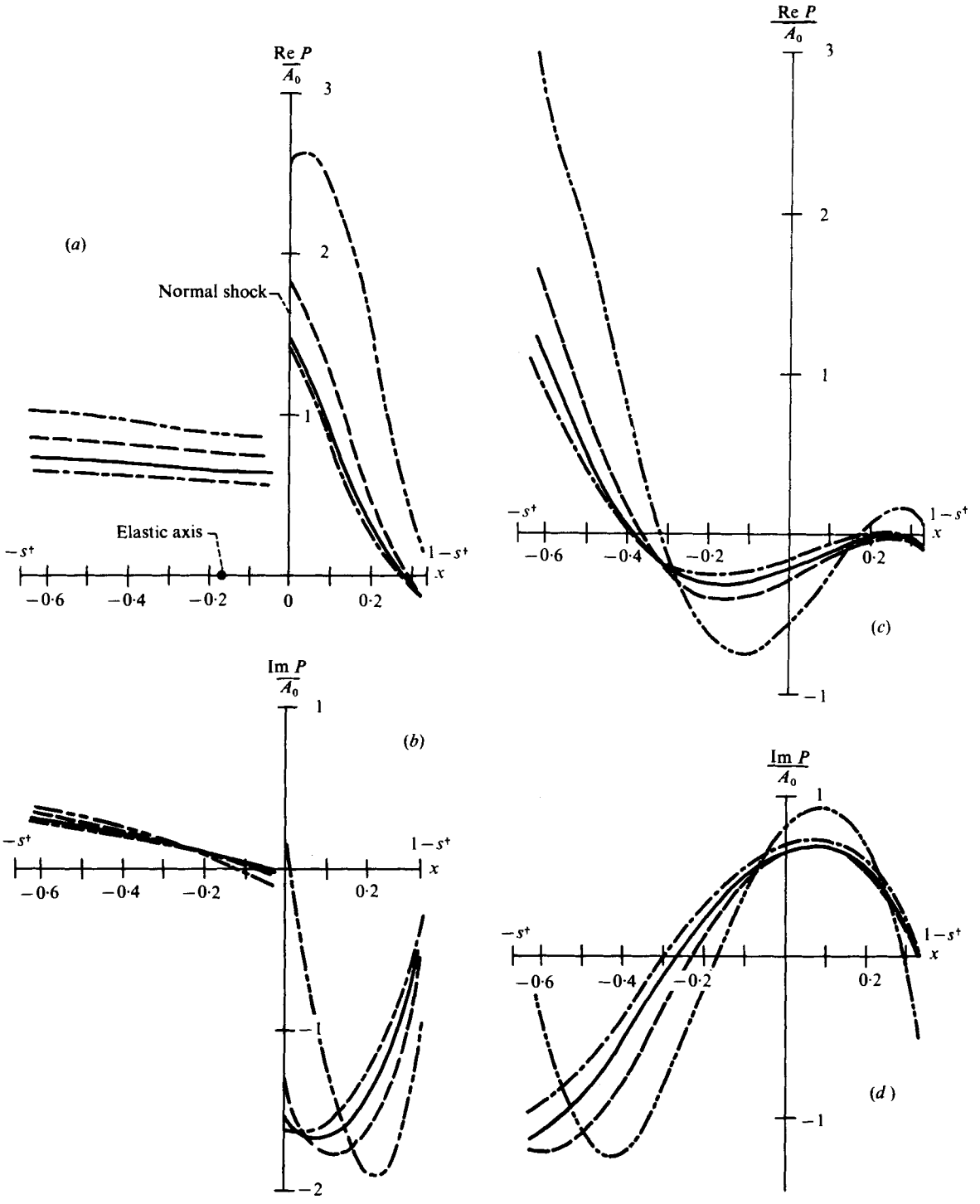

FIGURE 10. Non-dimensional surface pressure amplitudes acting on a cascade undergoing a pure pitching oscillation about the centre of the blades. Stagger angle = 60°; solidity = 1·3; interblade phase angle $\sigma = 0$; reduced frequency $\frac{1}{2}\omega_1 = 0{\cdot}5$. (*a*)–(*d*) and curves as in figure 9.

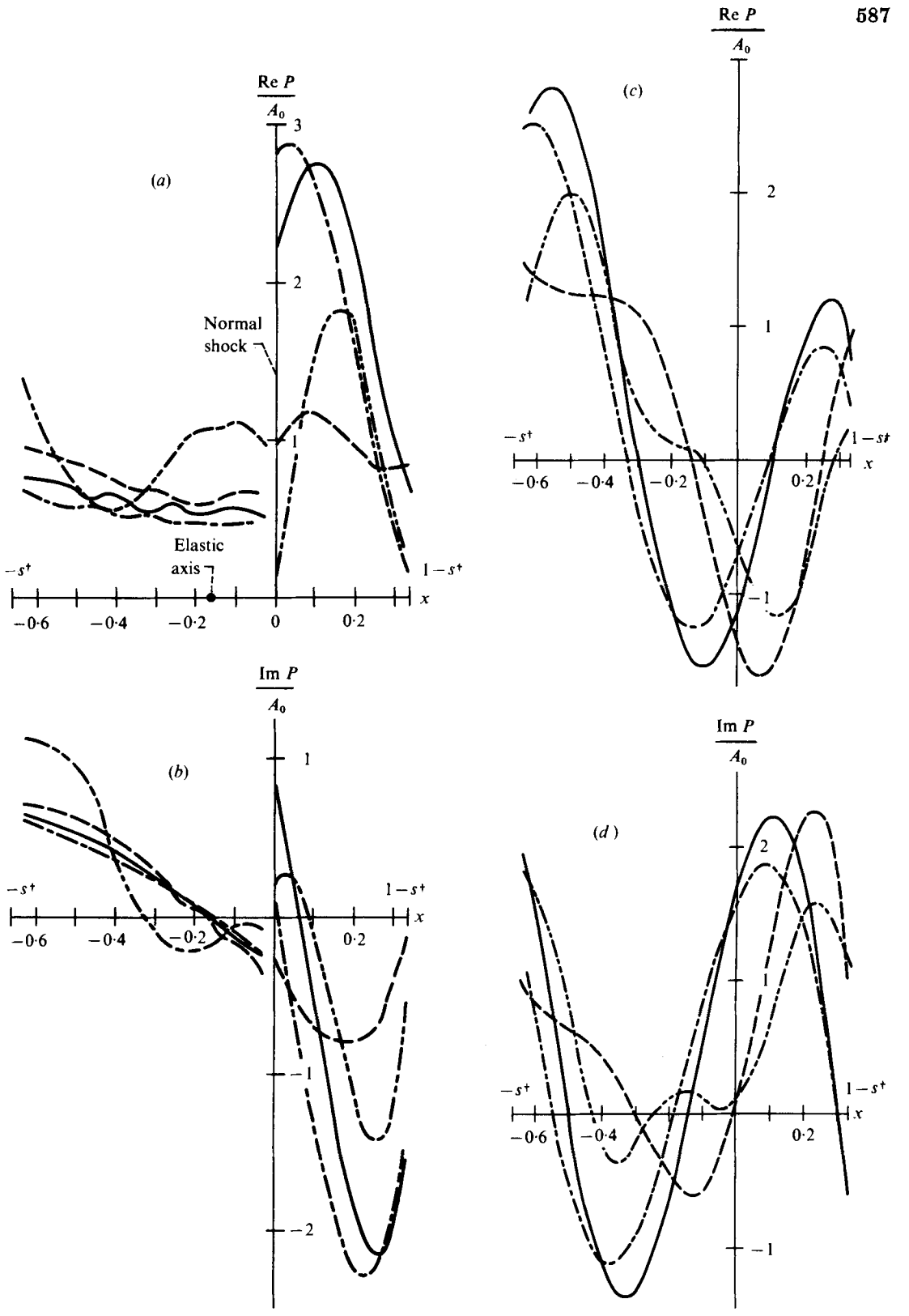

FIGURE 11. Non-dimensional surface pressure amplitudes acting on a cascade undergoing a pure pitching oscillation about the centre of the blades. Stagger angle = 60°; solidity = 1·3; inter-blade phase angle $\sigma = 0$; reduced frequency $\frac{1}{2}\omega_1 = 1$. (*a*)–(*d*) and curves as in figure 9.

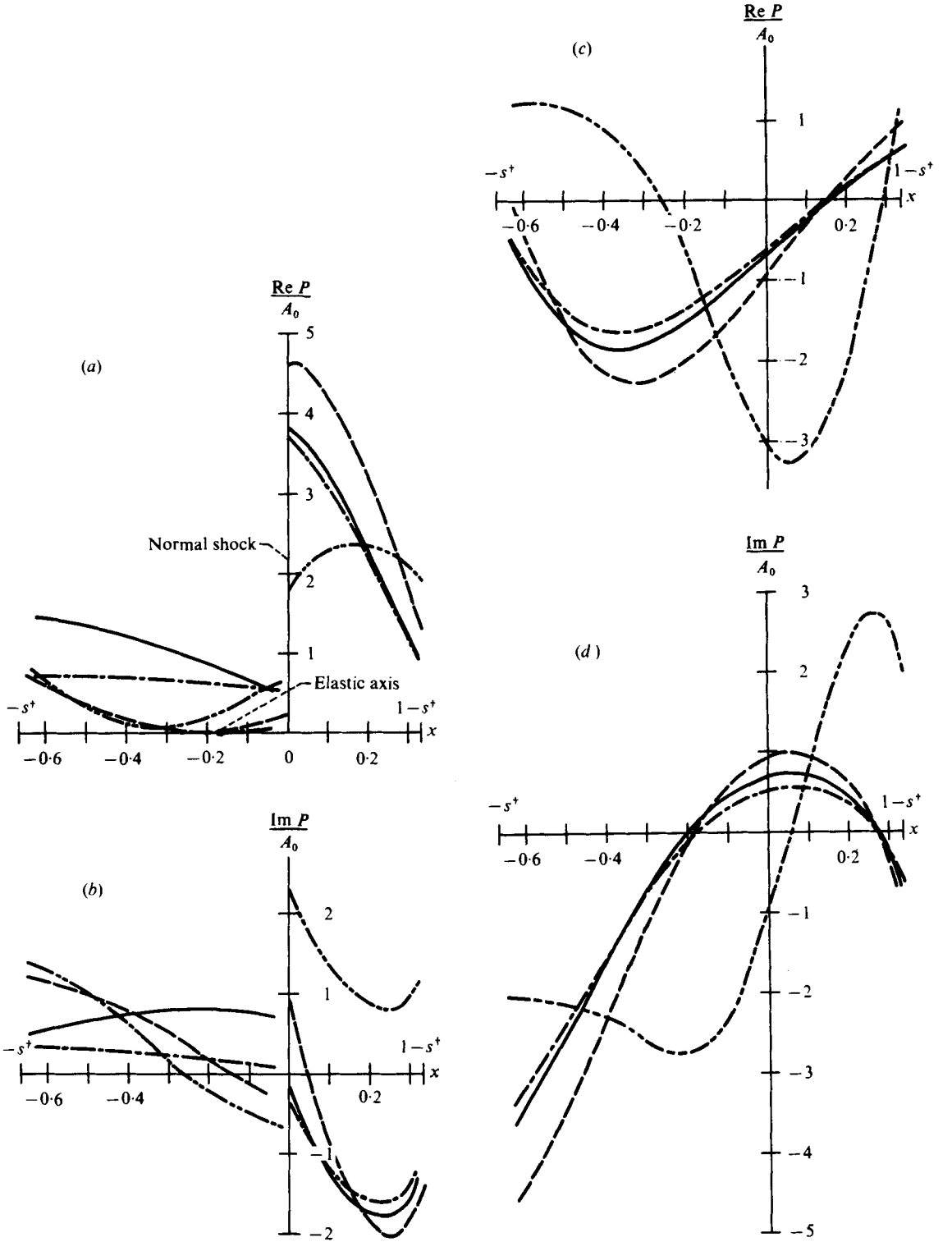

FIGURE 12. Non-dimensional surface pressure amplitudes acting on a cascade undergoing a pure pitching oscillation about the centre of the blades. Stagger angle = 60°; solidity = 1·3; inter-blade phase angle $\sigma = \frac{1}{2}\pi$; reduced frequency $\frac{1}{2}\omega_1 = 0{\cdot}5$. (*a*)–(*d*) and curves as in figure 9.

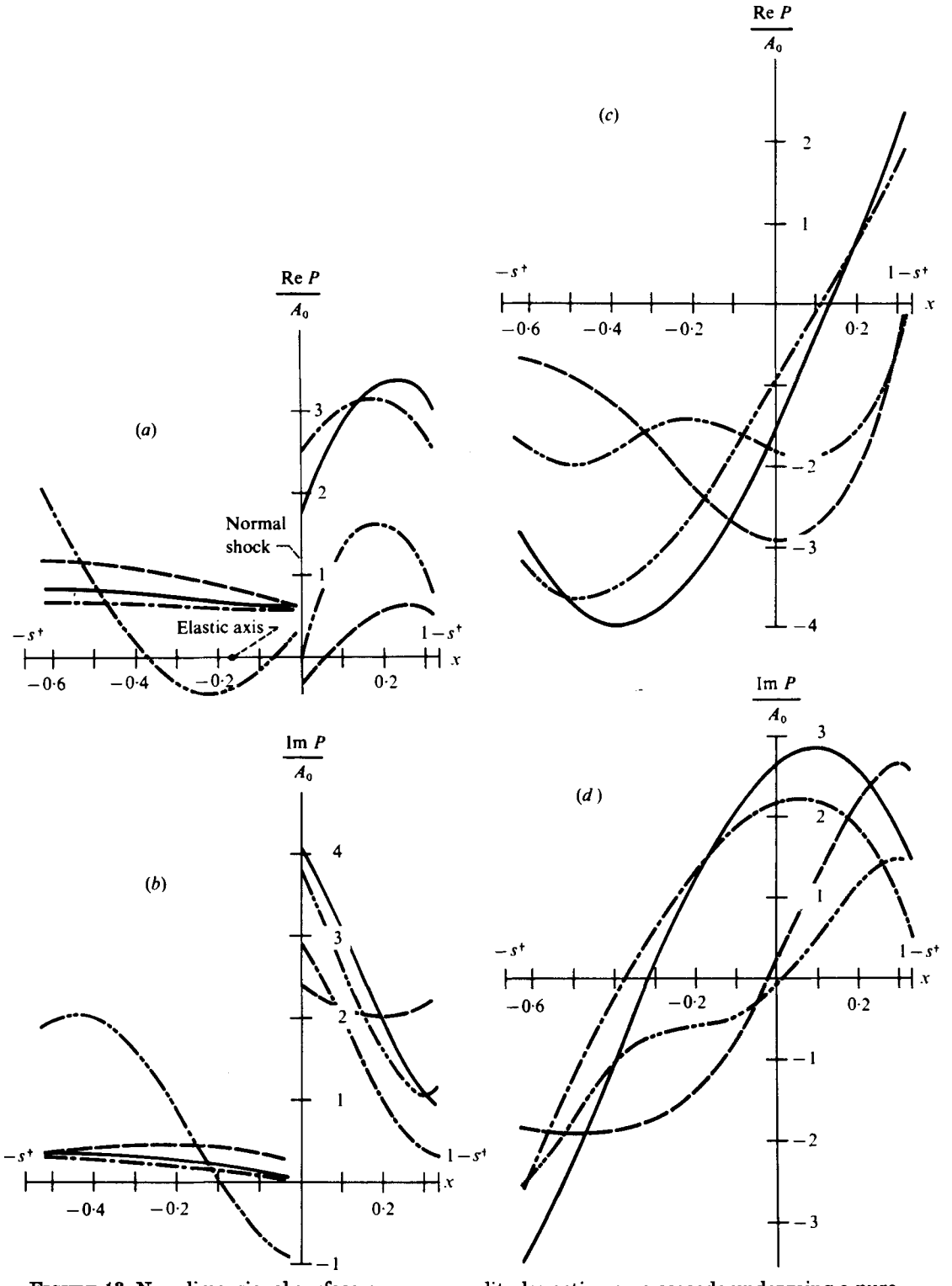

FIGURE 13. Non-dimensional surface pressure amplitudes acting on a cascade undergoing a pure pitching oscillation about the centre of the blades. Stagger angle = 60°; solidity = 1·3; inter-blade phase angle $\sigma = \pi$; reduced frequency $\frac{1}{2}\omega_1 = 0{\cdot}5$. (*a*)–(*d*) and curves as in figure 9.

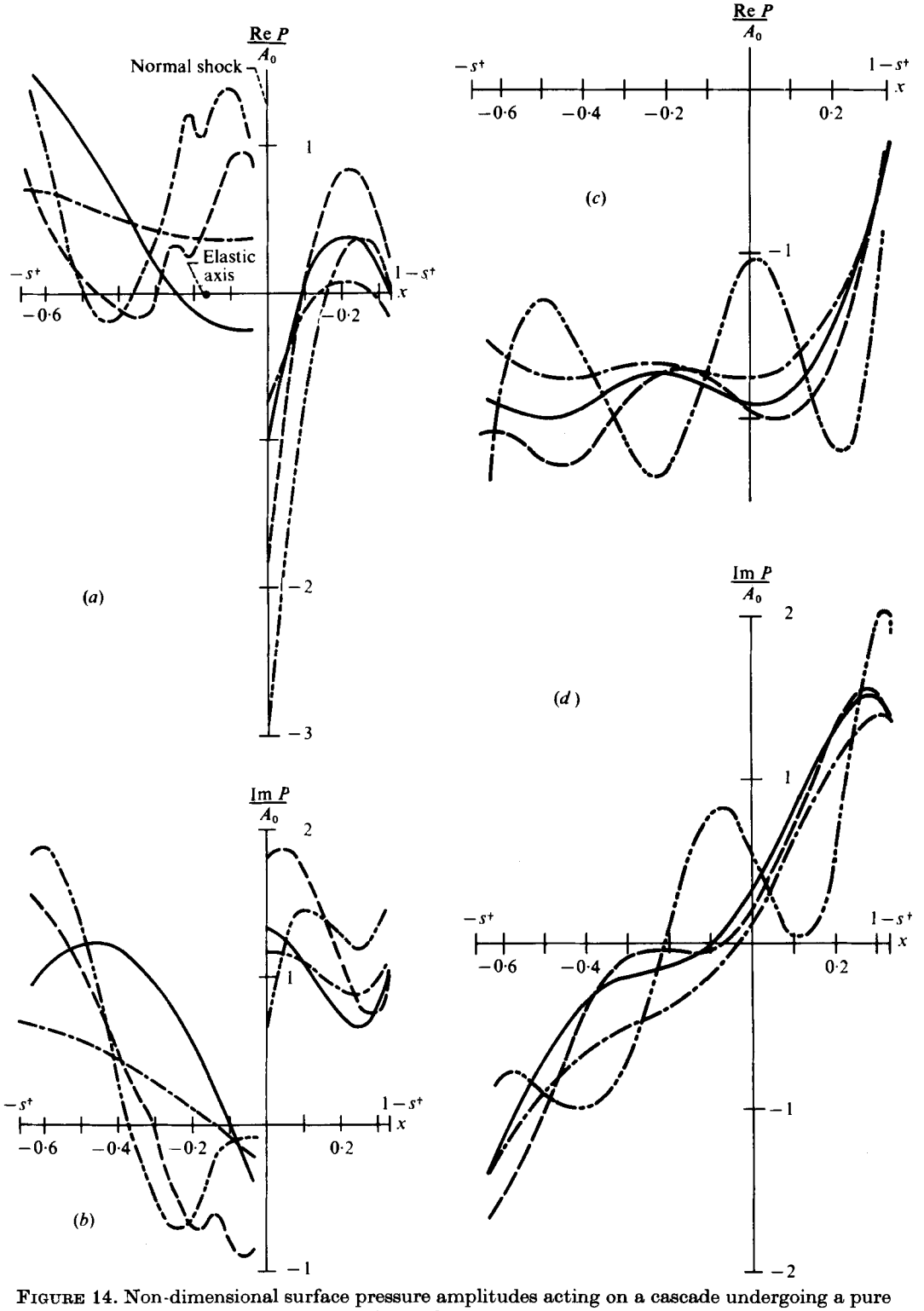

FIGURE 14. Non-dimensional surface pressure amplitudes acting on a cascade undergoing a pure pitching oscillation about the centre of the blades. Stagger angle = 60°; solidity = 1·3; inter-blade phase angle $\sigma = \pi$; reduced frequency $\frac{1}{2}\omega_1 = 1$. (*a*)–(*d*) and curves as in figure 9.

vary in a complicated fashion as these parameters are changed. Nevertheless, there do appear to be certain trends that can be deduced from the results.

The pressure distributions on the supersonic portion of the blade seem to exhibit the simplest behaviour. Notice that they tend to be fairly constant over the entire supersonic region at the lower reduced frequencies and higher Mach numbers. Under these conditions the pressures are relatively insensitive to the Mach number until $M_1 \to 1{\cdot}2$. Their behaviour then depends to a large extent on the interblade phase angle. When $\sigma = 0$ the overall pressure levels always increase with decreasing Mach number. But when $\sigma = \pi$ this behaviour is exhibited only at the lower reduced frequencies. As the reduced frequency is increased the supersonic pressure distributions become increasingly oscillatory. The same trend is observed with an isolated airfoil oscillating in a supersonic flow. Finally, it should be pointed out that the pressure distributions agree with those obtained by Verdon & McCune (1975) for a completely supersonic cascade.

Notice that the supersonic surface pressure is determined by a different set of equations in each of the regions $x \lessgtr -s\beta_1$. Nevertheless the results show that it always varies smoothly across the boundary of these two regions. Such behaviour is, of course, required by the physics of the problem since the pressure on the supersonic portion of the blade can only change discontinuously across Mach waves that emanate from the leading edges of the blades and extend downstream, while it is clear from figure 3 that no such Mach wave can intersect the supersonic portion of the upper surface of the blade.

The in-passage shock waves cause the pressure distributions on the subsonic portion of the blades to be considerably different from those that occur in a completely subsonic cascade. As indicated in the introduction, these shocks can affect the subsonic flow by transmitting and reflecting pressure waves as well as by generating downstream-propagating vorticity. Since the disturbances originating in the downstream region are reflected but not transmitted while the converse is true for upstream disturbances, it is not surprising that the surface pressure variations in the subsonic region are considerably more complex than those in the supersonic region. However, it again appears that certain consistent trends can be detected. Thus in most cases the absolute magnitude of the pressure on the upper surface appears to rise as the shock wave is approached. This behaviour is more pronounced at the lower reduced frequencies and higher Mach numbers. On the other hand, the pressure always takes on a finite value at the surface of the shock. In fact, unlike the purely subsonic cascade the pressures in the present problem are finite everywhere. However, the low frequency pressure amplitudes do show a tendency to become fairly large in the vicinity of the shock waves. Naturally the pressure on the upper surface is discontinuous across the shock position while that on the lower surface varies continuously across this region.

At low frequencies the real parts (in-phase components) of the pressures on the lower surface tend to be concave upwards while their imaginary parts tend to be concave downwards. This trend is masked by the oscillatory character of the solutions at the higher reduced frequencies.

As in the supersonic region, the upper surface pressures show a definite penchant for increasing with decreasing Mach number when the reduced frequency is low and the interblade phase angle is less than π. They also exhibit a tendency to increase in complexity as the reduced frequency increases or the interblade phase angle approaches π.

Finally, it should be noted that, as required by the Kutta condition, the upper and lower surface pressures become equal at the trailing edge. Since pressure signals from the trailing edge are now prevented from propagating all the way upstream, the physical mechanism that produces this effect is probably somewhat different from the one that causes it to occur in completely subsonic flows. Thus if at any instant a large gradient is set up because the trailing streamline does not emanate from the trailing edge of the blade, there can be no adjustment of the flow in the supersonic region to remedy the situation. However, pressure signals can be sent up to the normal shock, causing it to emit vorticity waves that change the circulatory flow in the subsonic region enough to move the trailing streamline back to the trailing edge of the blade and thereby prevent a pressure discontinuity from occurring at this point. In fact, since the circulation around the blade is just the line integral of the surface velocity, a movement of the shock–blade intersection point by an amount $x_s(0,t)$ causes the circulation to change by an amount

$$\gamma_s = (\mathscr{U}_1 - \mathscr{U}_2) x_s(0,t) c. \tag{4.1}$$

4.2. *Lift and moments: stability of cascade*

The contribution of the unsteady surface pressures to the fluctuating lift or moment can be calculated in the usual way by integrating these pressures (or their moments) over the surface of the blades. However, in the present problem there is an additional contribution to the fluctuating lift or moment that arises directly from the motion of the shock wave. Thus, owing to the oscillation of the shock, the length of the upper $n = 0$ blade surface that is in the supersonic region changes continuously by the amount $x_s(0,t)$ where, as indicated in appendix A, $x_s(0,t)$ denotes the dimensionless displacement of the shock wave at the upper surface of the $n = 0$ blade. The resulting lift force acting on the blade is therefore $x_s(0,t)[p_2^{(0)} - p_1^{(0)}]$, where $p_1^{(0)}$ and $p_2^{(0)}$ denote the steady pressures in regions 1 and 2. Then since it follows from the harmonic time dependence of the problem that $\partial x_s/\partial t = -i\omega x_s$, we can use equation (A 1*a*) to eliminate x_s and thereby show that $\mathscr{L}_s$, the amplitude of the shock-induced lift fluctuations non-dimensionalized by $c\rho_1 \mathscr{U}_1^2$, is given by

$$\mathscr{L}_s = \frac{i}{2k_1 M_1}\left[\frac{2M_1^2 - \mu + 1}{\mu + 1} P_1(0,0+) + \frac{4}{\mu+1} U_1(0,0+) - P_2(0,0+)\right],$$

where we have used the steady-state normal-shock relation

$$(p_2^{(0)} - p_1^{(0)})/\rho_1 \mathscr{U}_1^2 = 2\beta_1^2/[(\mu+1)M_1^2]$$

to eliminate the steady pressures (Shapiro 1953). This force will, of course, produce a moment about the point $x = d_0$ that has dimensionless amplitude $d_0 \mathscr{L}_s$.

We shall suppose that the equilibrium position of the shock is slightly ahead of the leading edge of the upper blade. Then there will be no contribution to the fluctuating lift from the motion of its footprint on the lower surface.

It is worth noting that the shock-induced circulation γ_s, given by (4.1), is related to the shock-induced lift fluctuation by

$$\rho_1 \mathscr{U}_1 \gamma_s = (\rho_1 \mathscr{U}_1^2 c \mathscr{L}_s e^{-i\omega t}).$$

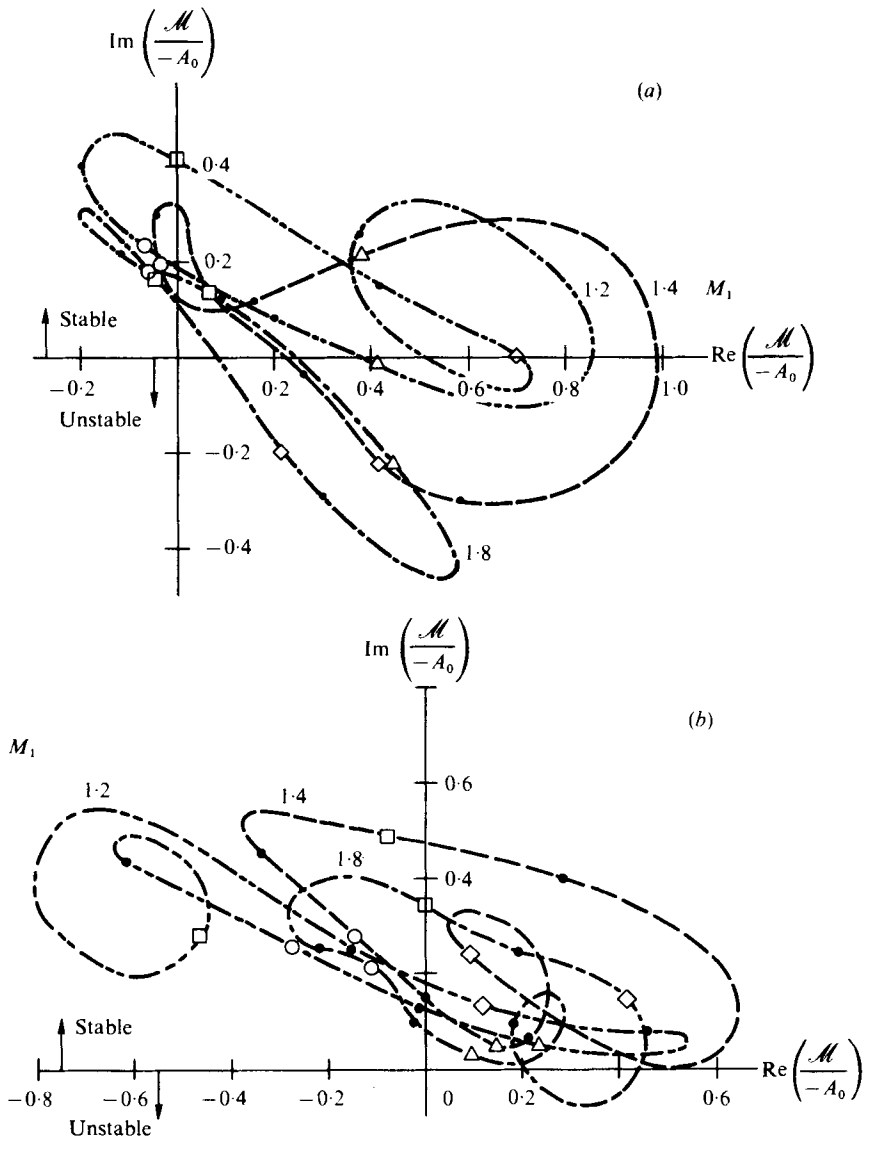

FIGURES 15 (*a*, *b*). For legend see next page.

Since the term on the right is just the actual dimensional shock-induced lift force, this result will be recognized as the familiar relation that connects the lift and circulation in potential flow theory.

The dimensionless moment coefficient [see 3.1 for description of $[\ ]_0$]

$$\mathscr{M} = \int_{-s\dagger}^{1-s\dagger} (x - d_0)[P]_0 \, dx + d_0 \mathscr{L}_s$$

divided by $-A_0$, the instantaneous angle of attack (assumed positive in the clockwise direction), is plotted for pure torsional (i.e. pitching) motion about the centre of the

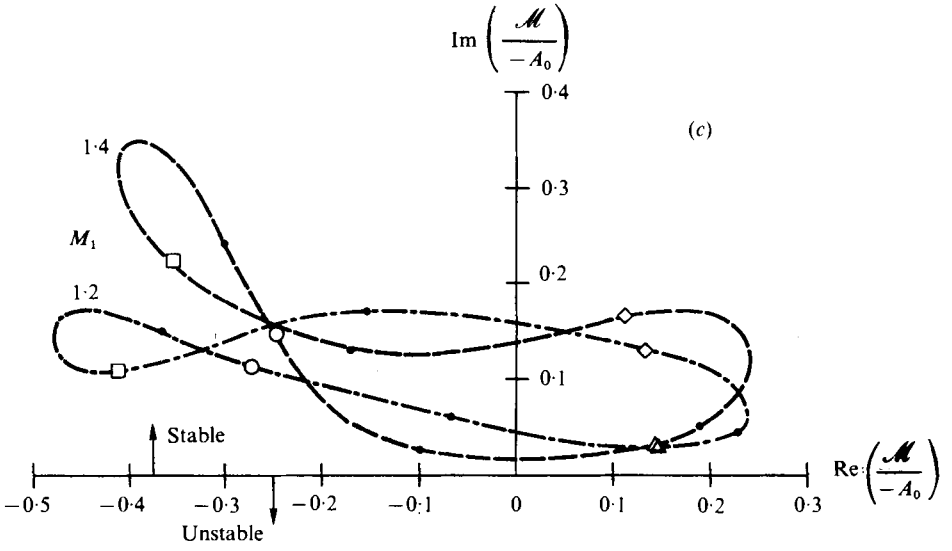

FIGURE 15. Moment coefficient for pitching motion about centre of blade. (Cascade geometry same as in figures 9–14.) ○, $\sigma = 0$; □, $\sigma = \frac{1}{2}\pi$; ◇, $\sigma = \pi$; △, $\sigma = \frac{3}{2}\pi$; ●, intermediate values of σ (i.e. multiples of $\frac{1}{4}\pi$). Reduced frequency $\frac{1}{2}\omega_1$: (*a*) 0·25; (*b*) 0·5; (*c*) 1.

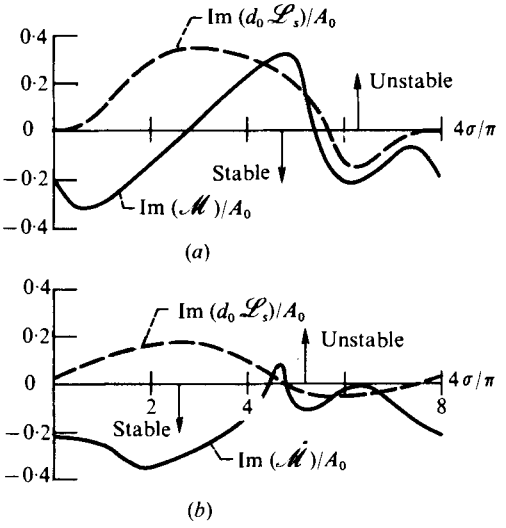

FIGURE 16. Effect of shock-induced moment on torsional stability.
(*a*) $M_1 = 1{\cdot}4$, $\omega_1 = 0{\cdot}5$. (*b*) $M_1 = 1{\cdot}8$, $\omega_1 = 1$.

blade (so that $d_0 = \frac{1}{2} - s^\dagger$) in figures 15(*a*)–(*c*). The interblade phase angle is taken as a parameter along the curve. The cascade configuration is the same as the one considered in the previous section. For torsional motion, the work per cycle (done *by* the flow *on* the blades) is equal to $\pi A_0 \rho_1 \mathscr{U}_1^2 \operatorname{Im} \mathscr{M}$ (Fung 1955). When this quantity is positive, the blade receives energy from the flow and thereby becomes unstable. Hence the cascade will flutter when $\operatorname{Im}(\mathscr{M}/-A_0)$ is negative. Figure 15 shows that the blade row is more stable at higher reduced frequencies and that the degree of

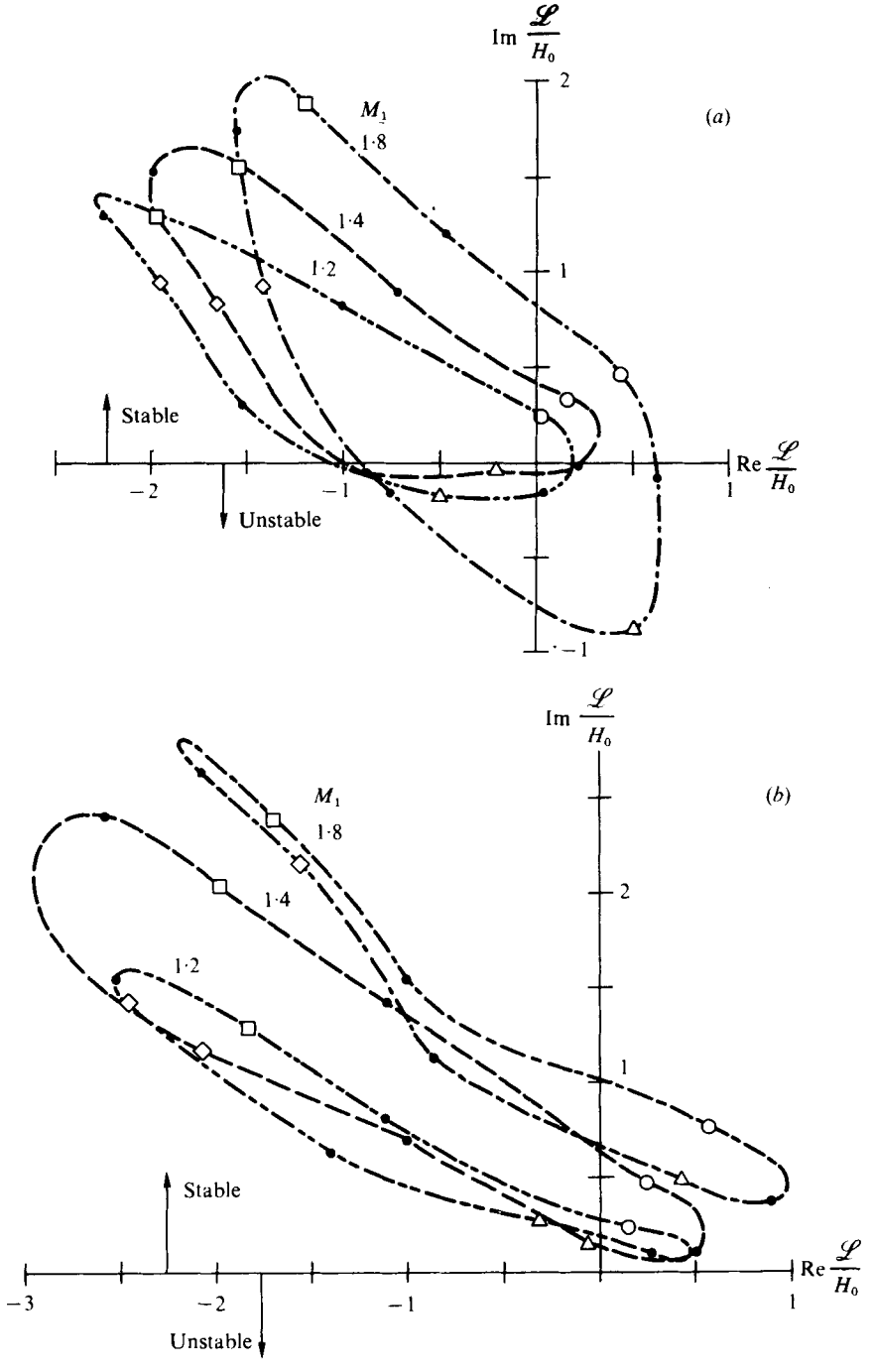

FIGURE 17. Lift coefficient for plunging motion. (Cascade geometry is same as in figures 9–14.) Symbols as in figure 15. Reduced frequency $\frac{1}{2}\omega_1$: (*a*) 0·25; (*b*) 0·5.

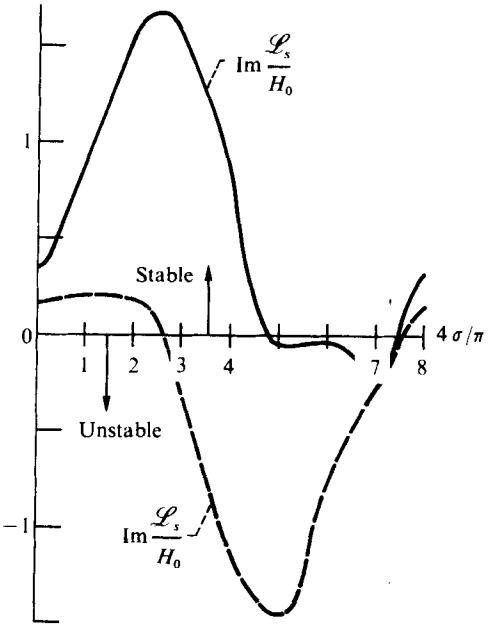

FIGURE 18. Effect of shock-induced lift on bending stability. $M_1 = 1{\cdot}4$, $\omega_1 = 0{\cdot}5$.

instability usually increases with Mach number. These results are somewhat similar to the calculations for a supersonic cascade of Verdon & McCune (1975). However, the present results exhibit a greater degree of stability in the sense that the portions of the curves extending below the real axis are smaller at any given reduced frequency while complete stability at any given Mach number (for all values of the interblade phase angle) occurs at a much lower reduced frequency. Not unexpectedly, the response curves have a somewhat more complex shape than those for a completely supersonic cascade.

The fact that the present calculation predicts greater stability than the completely supersonic model (which represents the real flow only at low backpressures) is consistent with the increase in torsional stability that is found to occur in virtually all fans and compressors when the backpressure is increased.

In figure 16 the imaginary part of the shock-induced fluctuating moment is compared with the imaginary part of the total moment. These results are typical in that (for all cases considered) the shock-induced moment tends to be destabilizing for interblade phase angles in the range $0 < \sigma < \frac{5}{4}\pi$ and stabilizing for interblade phase angles outside this range. Instability of the blade always seems to occur in a region where the shock-induced moment is destabilizing. In fact, the shock moment usually acts to decrease the overall stability of the cascade. Hence it cannot be responsible for the increased stability exhibited by the present model (as compared with the purely supersonic cascade model). There does not appear to be any consistent Mach number effect.

The dimensionless lift

$$\mathscr{L} = -\int_{s\dagger}^{1-s\dagger} [P]_0 dx + \mathscr{L}_s$$

is plotted in figures 17(*a*) and (*b*), for the case of pure bending (i.e. plunging motion). The geometry of the cascade is the same as before. The figures show that the blades become unstable at the lower frequencies (below $\frac{1}{2}\omega_1 \simeq 0{\cdot}3$) and that the degree of instability increases with Mach number. Corresponding calculations for the purely supersonic cascade (Kurosaka 1974; Verdon & McCune 1975) indicate that the blades will always be stable. However, recent supersonic compressor tests have revealed that bending flutter will occur at the higher backpressures whenever $\frac{1}{2}\omega_1$ is less than 0·3.

The imaginary part of the shock-induced lift fluctuation is compared with the overall lift fluctuation in figure 18. These curves are again typical in that they show the shock-induced lift to be primarily stabilizing for interblade phase angles in the range $0 < \sigma < \frac{1}{2}\pi$ and destabilizing in the range $\frac{1}{2}\pi < \sigma < \pi$. Since the calculations indicate that bending flutter always occurs in the latter range it may be possible to attribute the bending instability of the blade row to the destabilizing force induced by the shock waves.

5. Concluding remarks

We have developed a linearized theory for predicting the unsteady flow in supersonic cascades containing in-passage shocks. Our model accounts for not only the direct shock-induced fluctuating blade forces but also those due to the shock reflected pressure waves. The direct shock forces are found to be predominantly destabilizing for both pitching and plunging motion and can therefore not be responsible for producing the increase in torsional stability exhibited by the present calculation. However, they may be responsible for producing the supersonic bending flutter that has been found in recent compressor tests.

Unlike the case where the flow is everywhere subsonic, it is possible in the present problem to impose a Kutta condition at the trailing edge without causing the pressure to become infinite at some other point. This may be a reflexion of the fact that the physical mechanism that causes the flow to satisfy the Kutta condition is not the same as the one that causes this condition to hold in a completely subsonic flow.

Thanks are due to Jon Kring for carrying out the numerical computations. The authors are indebted to John Caruthers (Detroit Disel Allison) for bringing the shock-induced forces to their attention.

Appendix A

In this appendix we derive conditions connecting the flow across the shock waves. A convenient starting point is the set of conditions derived by Moore (1954). His results can be written as

$$\left.\begin{aligned} p_2' &= \left(\frac{2M_1^2-\mu+1}{\mu+1}\right)p_1' + \frac{4}{\mu+1}\left(u_1 - \frac{\partial x_s}{\partial t}\right), && \text{(A 1}a\text{)}\\ u_2 - \frac{\partial x_s}{\partial t} &= \left[\frac{(\mu-1)M_1^2-2}{(\mu+1)M_1^2}\right]\left(u_1-\frac{\partial x_s}{\partial t}\right) + 2\left(\frac{\mu-1}{\mu+1}\right)p_1', && \text{(A 1}b\text{)}\\ v_2 - v_1 &= \left(1-\frac{\mathscr{U}_2}{\mathscr{U}_1}\right)\frac{\partial x_s}{\partial y}, && \text{(A 1}c\text{)} \end{aligned}\right\} \quad \begin{array}{l} x = ns^{\dagger},\\ sn < y < (n+1)s\\ (n = 0, \pm 1, \pm 2, \ldots), \end{array}$$

where $x_s(y,t)$ denotes the dimensionless x-direction displacement of the shock waves measured from their equilibrium (i.e. steady-state) positions. It is assumed that this displacement will be of the same order as the perturbation quantities (p_1', p_2', u_2, etc.).

Since

$$v_1 = \partial\phi_1/\partial y, \quad v_2 = \partial\phi_2/\partial y - \partial\psi_2/\partial x, \quad \partial\phi_1/\partial t = -p_1' - u_1$$

and

$$\partial\phi_2/\partial t = -(\mathscr{U}_2/\mathscr{U}_1)(p_2' + u_2 - \partial\psi_2/\partial y),$$

(A 1c) can be differentiated with respect to time to obtain

$$\frac{\partial}{\partial y}\left[\left(p_1' + u_1 - \frac{\partial x_s}{\partial t}\right) - \frac{\mathscr{U}_2}{\mathscr{U}_1}\left(p_2' + u_2 - \frac{\partial x_s}{\partial t}\right)\right] = -\left(\frac{\mathscr{U}_2}{\mathscr{U}_1}\frac{\partial^2\psi_2}{\partial y^2} + \frac{\mathscr{U}_1}{\mathscr{U}_2}\frac{\partial^2\psi_2}{\partial t^2}\right).$$

Then substituting in (A 1a,b) and using the well-known normal-shock relation (see Crocco 1954, p. 111) $\mathscr{U}_2/\mathscr{U}_1 = [(\mu-1)M_1^2+2]/[(\mu+1)M_1^2]$ together with (2.7) yields

$$\frac{\partial}{\partial y}\left[p_2' - \left(M_1^2 + \frac{\mu-1}{\mu+1}\beta_1^2\right)p_1'\right] = -(\mu+1)\left(\frac{M_1 M_2}{\beta_1\beta_2}\right)^2\left(\frac{\partial^2\psi_2}{\partial y^2} + \frac{\mathscr{U}_1^2}{\mathscr{U}_2^2}\frac{\partial^2\psi_2}{\partial t^2}\right). \tag{A 2}$$

On the other hand (A 1a,b) imply

$$u_2 = -\frac{M_1^2+1}{2M_1^2}p_2' + u_1 + \frac{1}{2}\left[M_1^2 + 1 - \frac{\beta_1^4}{M_1^2}\left(\frac{\mu-1}{\mu+1}\right)\right]p_1'$$

$$\text{for} \quad x = ns, \quad sn < y < (n+1)s \quad (n = 0, \pm 1, \pm 2, \ldots). \tag{A 3}$$

Appendix B

In this appendix we use the Wiener–Hopf method to solve the dual integral equations (3.11) and (3.12). It is shown in Noble (1958, pp. 220 ff.) that these equations are equivalent to the functional equations

$$X_+(\alpha)\kappa_1(\alpha,0) = X_-(\alpha) + F_+(\alpha) \quad \text{for} \quad -\infty < \mathrm{Re}\,\alpha < \infty, \quad \mathrm{Im}\,\alpha = \epsilon_1 M_1, \tag{B 1}$$

where $X_+(\alpha)$ is a function which is analytic in the upper half-plane $\mathrm{Im}\,\alpha > M_1\epsilon_1$, $X_-(\alpha)$ is analytic in the lower half-plane $\mathrm{Im}\,\alpha < M_1\epsilon_1$,

$$f_0^{(1)}(\alpha) = X_+(\alpha) \quad \text{for} \quad -\infty < \mathrm{Re}\,\alpha < \infty, \quad \mathrm{Im}\,\alpha = \epsilon_1 M_1 \tag{B 2}$$

and

$$F_+(\alpha) \equiv \int_0^\infty \exp\{i(\alpha - M_1 k_1)\tilde{x}_1\}\left(\frac{\partial}{\partial\tilde{x}_1} - i\omega_1\right)W_0(\tilde{x}_1 - s^\dagger)\,d\tilde{x}_1. \tag{B 3}$$

Equation (B 1) is solved by first factorizing $\kappa_1(\alpha,0)$ into the product

$$\kappa_1(\alpha,0) = \kappa_1^+(\alpha)/\kappa_1^-(\alpha), \quad \mathrm{Im}\,\alpha = \epsilon_1 M_1, \tag{B 4}$$

where $\kappa_1^+(\alpha)$ is analytic and non-zero in the upper half-plane and remains bounded as $\alpha\to\infty$ while $\kappa_1^-(\alpha)$ is analytic and non-zero in the lower half-plane and is bounded as $\alpha\to\infty$ in this region. We next factorize $\kappa_1^-(\alpha)F_+(\alpha)$ into the difference

$$G_+(\alpha) - G_-(\alpha) = \kappa_1^-(\alpha)F_+(\alpha), \quad \mathrm{Im}\,\alpha = \epsilon_1 M_1, \tag{B 5}$$

where $G_+(\alpha)$ is analytic and has algebraic behaviour at infinity in the upper half-plane while $G_-(\alpha)$ is analytic and has algebraic behaviour at infinity in the lower half-plane. Then (B 1) becomes

$$X_+(\alpha)\kappa_1^+(\alpha) - G_+(\alpha) = X_-(\alpha)\kappa_1^-(\alpha) - G_-(\alpha), \quad -\infty < \mathrm{Re}\,\alpha < \infty, \quad \mathrm{Im}\,\alpha = \epsilon_1 M_1.$$

The left-hand side of this result is the boundary value of a function that is analytic in the upper half-plane and the right-hand side is the boundary value of a function that is analytic in the lower half-plane, so that these two functions are analytic continuations of one another and together define an entire function. Moreover, by using the known relations between the asymptotic expansion for large α of the various Fourier transforms and the behaviour of the physical variables near $\tilde{x}_1 = 0$, it can be shown that the latter quantities will remain bounded at this point only if the left- and right-hand sides of this equation vanish in their appropriate half-planes as $\alpha \to \infty$. Hence it follows from Liouville's theorem that each side must vanish identically and therefore that (B 2) becomes

$$f_0^{(1)}(\alpha) = G_+(\alpha)/\kappa_1^+(\alpha). \tag{B 6}$$

In order to determine G_+ from (B 5), we must evaluate the integral (B 3). The function W_0 is given by (2.16) for $\tilde{x}_1$ in the range $0 < \tilde{x}_1 < s^\dagger$ while its definition in the range $s^\dagger < \tilde{x}_1$ will not affect the solution in region 1. We should therefore define this function such that we obtain the simplest possible solution to (B 5). This will occur when the definition (2.16) is extended into the region $s^\dagger < \tilde{x}_1$. But this procedure will lead to divergent integrals unless we replace the boundary condition (2.16) by the slightly modified condition

$$W_0 = [H_0 + A_0(x - d_0)] \exp(-\epsilon_0 \tilde{x}_1), \tag{B 7}$$

where $0 < \epsilon_0 \ll 1$. This formula represents an oscillatory surface motion that slowly decays as $x \to \infty$.

At the end of the problem, we can put $\epsilon_0 = 0$ and the final solution will not diverge as long as we restrict our attention to region 1. This procedure allows us to locate the poles on the correct side of the integration contour.

Thus inserting (B 7) into (B 3) and carrying out the integration shows that

$$F_+(\alpha) = \frac{iA_0 + \omega_1[H_0 - A_0(s^\dagger + d_0)]}{\alpha - M_1 k_1 + i\epsilon_0} + \frac{i\omega_1 A_0}{(\alpha - M_1 k_1 + i\epsilon_0)^2}$$

and on inserting this into (B 5) we find by inspection that

$$G_+(\alpha) = \frac{\kappa_1^-(M_1 k_1 - i\epsilon_0)}{\alpha - M_1 k_1 + i\epsilon_0} \left(D_- + i\omega_1 \frac{A_0}{\alpha - M_1 k_1 + i\epsilon_0} \right),$$

where

$$D_- \equiv iA_0 \left\{ 1 + \omega_1 \frac{[\kappa_1^-(M_1 k_1 - i\epsilon_0)]'}{\kappa_1^-(M_1 k_1 - i\epsilon_0)} \right\} + \omega_1[H_0 - A_0(s^\dagger + d_0)] \tag{B 8}$$

and

$$[\kappa_1^-(x)]' \equiv d\kappa_1^-(x)/dx. \tag{B 9}$$

Equation (B 6) can therefore be written as

$$f_0^{(1)} = \frac{\kappa_1^-(M_1 k_1 - i\epsilon_0)}{\kappa_1^+(\alpha)(\alpha - M_1 k_1 + i\epsilon_0)} \left(D_-^{(1)} + \frac{i\omega_1 A_0}{\alpha - M_1 k_1 + i\epsilon_0} \right). \tag{B 10}$$

Appendix C

In this appendix, we solve the functional equation (B 4). Substituting (3.8) into (3.10) and carrying out the differentiation shows after some rearrangement that

$$\kappa_1(\alpha, 0) = \beta_1 \gamma_1 \sin(\beta_1 \gamma_1 s)/(2 \sin \Delta_1^+ \sin \Delta_1^-). \tag{C 1}$$

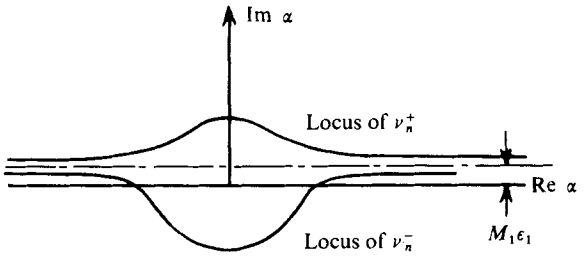

FIGURE 19. Approximate locus of roots in complex α plane.

The numerator of this equation has its zeros at the points where $\beta_1\gamma_1 s = n\pi$ for $n = 0, \pm 1, \pm 2, \ldots$, i.e. at the points

$$\lambda_n^{(1)} = [k_1^2 + (n\pi/(\beta_1 s))^2]^{\frac{1}{2}} \quad \text{for} \quad n = 0, \pm 1, \pm 2, \ldots . \tag{C 2}$$

But these points all lie below the line $\mathrm{Im}\,\alpha = \epsilon_1 M_1$ and hence belong to the lower half-plane. We can therefore conclude that the numerator of (C 1) is analytic and non-zero in the upper half-plane and can as a consequence associate it with $\kappa_1^+(\alpha)$.

Since the equation immediately below (3.8) shows that replacing γ_1 by $-\gamma_1$ changes Δ_1^+ into Δ_1^- and vice versa, we can see that the denominator of (C 1) remains unchanged under this substitution. Hence it depends only on $\gamma_1^2 = \alpha^2 - k_1^2$ and consequently is an analytic function of α. However, it possesses zeros which lie both above and below the line $\mathrm{Im}\,\alpha = \epsilon_1 M_1$. In order to sort these out, we use the well-known result (based on the Weierstrass factorization formula)

$$\sin\alpha = \alpha \prod_{n=1}^{\infty} \left[1 - \left(\frac{\alpha}{n\pi}\right)^2\right]$$

to conclude that

$$\sin\Delta_1^+ \sin\Delta_1^- = \Delta_1^+ \Delta_1^- \prod_{\substack{n=-\infty \\ n\neq 0}}^{\infty} \frac{1}{n^2\pi^2} (\Delta_1^+ - n\pi)(\Delta_1^- - n\pi).$$

After some manipulation, this becomes

$$\sin\Delta_1^+ \sin\Delta_1^- = \left[\left(\frac{d_1^+}{2}\right)^2 \nu_0^+ \nu_0^- \prod_{\substack{n=-\infty \\ n\neq 0}}^{\infty} \left(\frac{d_1^+}{2n\pi}\right)^2 \nu_n^+ \nu_n^-\right] \left[\prod_{n=-\infty}^{\infty} \left(1 - \frac{\alpha}{\nu_n^-}\right)\right] \left[\prod_{n=-\infty}^{\infty} \left(1 - \frac{\alpha}{\nu_n^+}\right)\right], \tag{C 3}$$

where

$$d_1^+ = (s^{+2} - \beta_1^2 s^2)^{\frac{1}{2}}, \tag{C 4}$$

$$\nu_n^{\pm} = \Gamma_n^{(1)} \frac{s^+}{d_1^+} \pm \frac{s\beta_1}{d_1^+} ([\Gamma_n^{(1)}]^2 - k_1^2)^{\frac{1}{2}} \quad \text{for} \quad n = 0, \pm 1, \pm 2, \ldots, \tag{C 5}$$

$$\Gamma_n^{(1)} \equiv (2n\pi + M_1 k_1 s^+ - \sigma)/d_1^+ \tag{C 6}$$

and the branch cut for the square root is the one shown in figure 5. The loci of the points $\alpha = \nu_n^{\pm}$ are shown schematically in figure 19.

The first term in square brackets in (C 3) is a constant. Moreover, it follows from figure 19 that the second term in square brackets has its zeros at points in the lower

half-plane while the third term has its zeros in the upper half-plane. Hence we can conclude that

$$\kappa_1^+(\alpha) = e^{\chi(\alpha)}\frac{\beta_1\gamma_1}{2}\sin(\beta_1\gamma_1 s)\left[\left(\frac{d_1^\dagger}{2}\right)^2 \nu_0^+\nu_0^- \prod_{\substack{n=-\infty \\ n\neq 0}}^{\infty}\left(\frac{d_1^\dagger}{2n\pi}\right)^2 \nu_n^+\nu_n^-\right]^{-1}\left[\prod_{n=-\infty}^{\infty}\left(1-\frac{\alpha}{\nu_n^-}\right)\right]^{-1}$$

and

$$\kappa_1^-(\alpha) = e^{\chi(\alpha)}\prod_{n=-\infty}^{\infty}\left(1-\frac{\alpha}{\nu_n^+}\right),$$

where $\chi(\alpha)$ is an entire function of α that must be chosen in such a way that $\kappa_1^\pm$ remain bounded at infinity in the appropriate half-planes.

In order to evaluate this function we must first determine the asymptotic expansion of $\kappa_1^-(\alpha)$ as $\alpha\to\infty$. After a rather tedious calculation (following the procedure outlined in Noble 1958, p. 128, exercise 3.4) we find that

$$\kappa_1^-(\alpha) \sim \frac{e^{\chi(\alpha)}\sin[\frac{1}{2}(\alpha(s^\dagger-\beta_1 s)-M_1k_1s^\dagger+\sigma)]}{\sin[\frac{1}{2}(\sigma-M_1k_1s^\dagger)]}\prod_{n=-\infty}^{\infty}\frac{\Gamma_n^{(1)}d_1^\dagger}{\nu_n^+(s^\dagger-\beta_1 s)} \quad \text{as} \quad \alpha\to\infty.$$

Hence, in order to ensure that κ_1^- remains bounded as $\alpha\to\infty$ in the lower half-plane $-\pi+\epsilon < \arg\alpha < \epsilon$, we put $\chi = -\frac{1}{2}i\alpha(s^\dagger-\beta_1 s)$ so that

$$\kappa_1^-(\alpha) = \exp\left\{-i\left(\frac{s^\dagger-\beta_1 s}{2}\right)\alpha\right\}\prod_{n=-\infty}^{\infty}\left(1-\frac{\alpha}{\nu_n^+}\right) \tag{C 7}$$

and as $\alpha\to\infty$

$$\kappa_1^-(\alpha) \sim \kappa_\infty\{1-\exp\{-i[\alpha(s^\dagger-\beta_1 s)+\sigma-M_1k_1s^\dagger]\}\}, \tag{C 8}$$

where

$$\kappa_\infty \equiv \frac{-i\exp\{\frac{1}{2}i(\sigma-M_1k_1s^\dagger)\}}{2\sin[\frac{1}{2}(\sigma-M_1k_1s^\dagger)]}\prod_{n=-\infty}^{\infty}\frac{\Gamma_n^{(1)}d_1^\dagger}{\nu_n^+(s^\dagger-\beta_1 s)}.$$

Appendix D

In this appendix we use the solution (3.13) to calculate the airfoil surface pressure. The appropriate equation is obtained by substituting (3.13) into (2.5) and carrying out the indicated differentiation. The arguments made in connexion with the shock surface pressure can again be used to show that the singularities in the integrand of this result are at most poles. However, in this case, we find that the integration contour must be closed in the upper half-plane when x is in the range $-s^\dagger < x < -s\beta_1$ while it must be closed in the lower half-plane when x is in the range $-s\beta_1 < x < 0$.

The poles in the upper half-plane occur at the points ν_n^+ ($n = 0, \pm 1, \pm 2, \ldots$) defined by (C 5) and (C 6) while those in the lower half-plane occur at the same points as those in the integrands of the shock surface quantities. Hence, upon using the method of residues, we find that

$$P_1(x,0) = -is\sum_{n=-\infty}^{\infty}\frac{\nu_n^+-k_1/M_1}{\nu_n^+-M_1k_1}\frac{\kappa_1^-(M_1k_1)}{[\kappa_1^-(\nu_n^+)]'}\frac{\exp\{-i(\nu_n^+-M_1k_1)(x+s^\dagger)\}}{d_1^\dagger\Gamma_n^{(1)}-\nu_n^+s^\dagger} \times\left(D_-^{(1)}+\frac{i\omega_1A_0}{\nu_n^+-M_1k_1}\right) \quad \text{for} \quad -s^\dagger < x < -s\beta_1, \tag{D 1}$$

where ν_n^+ is defined by (C 4)–(C 6), κ_1^- is given by (C 7) and $[\kappa_1^-(x)]'$ is defined by (B 9). Similarly,

$$P_1(x,0) = \exp(iM_1k_1x)\sum_{n=0}^{\infty}(T_n^+\exp(-i\lambda_n^{(1)}x)+T_n^-\exp(i\lambda_n^{(1)}x)) - \omega_1^2[H_0+A_0(x-d_0)]f_1(0,M_1\omega_1)$$

$$-iA_0\left[\frac{\partial}{\partial\omega_1}\omega_1^2 f_1(0, M_1\omega_1)+\omega_1^2 f_2(0, M_1\omega_1)\right] \quad \text{for} \quad -s\beta_1 < x < 0, \tag{D 2}$$

where

$$T_n^{\pm} \equiv -[[\pm\lambda_n^{(1)}-(k_1/M_1)]/(\pm\lambda_n^{(1)}-M_1k_1)]Q_n^{\pm},$$

$\lambda_n^{(1)}$ is defined by (C 2) and f_1, f_2 and $Q_{ni}^{\pm}$ are defined by (3.19) and (3.17).

Appendix E

In this appendix we give the infinite-product representations for the factors $\kappa_2^{\pm}$ of the subsonic kernel function (3.26). The function κ_2^- is given by

$$\kappa_2^-(\alpha) = \frac{[\sin(s\beta_2k_2)](\alpha-k_2)\exp(i\alpha b/\pi)}{k_2[(\cos(s\beta_2k_2)-\cos(\sigma+M_2k_2s^{\dagger})](1-\alpha/\alpha_0^+)}\prod_{n=1}^{\infty}\frac{[1-(\alpha/\lambda_n^{(2)})]}{[1-(\alpha/\alpha_n^+)][1-(\alpha/\alpha_{-n}^+)]}, \tag{E 1}$$

where

$$\Gamma_n^{(2)} \equiv (2n\pi-\sigma-M_2k_2s^{\dagger})/d_2^{\dagger}, \tag{E 2}$$

$$d_2^{\dagger} \equiv (s^{\dagger 2}+\beta_2^2s^2)^{\frac{1}{2}}, \tag{E 3}$$

$$\alpha_n^{\pm} = \Gamma_n^{(2)}\frac{s^{\dagger}}{d_2^{\dagger}} \pm i\frac{s\beta_2}{d_2^{\dagger}}([\Gamma_n^{(2)}]^2-k_2^2)^{\frac{1}{2}} \tag{E 4}$$

are analogous to $\nu_n^{\pm}$, $\Gamma_n^{(1)}$ and $d_1^{\dagger}$ for the supersonic solution and

$$b \equiv s^{\dagger}[\tfrac{1}{2}\pi-\tan^{-1}(s\beta_2/s^{\dagger})]+s\beta_2\ln(2s\beta_2/d_2^{\dagger}).$$

The function κ_2^+ is given by

$$\kappa_2^+(\alpha) = \frac{(\alpha+k_2/M_2)(1-\alpha/\alpha_0^-)\exp(ib\alpha/\pi)}{\beta_2(\alpha+k_2)}\prod_{n=1}^{\infty}\frac{[1-(\alpha/\alpha_n^-)][1-(\alpha/\alpha_{-n}^-)]}{1+(\alpha/\lambda_n^{(2)})}. \tag{E 5}$$

Appendix F

After some algebraic manipulation the inhomogeneous term in (3.33) can be put in the form

$$\begin{aligned}F_n = {} & \frac{(1+\delta_{n,0})s}{2}a_n^-H_n\exp\{i\eta_n^-(s^{\dagger}-1)\}-\frac{(2M_2^2-\beta_2^2)}{\beta_2^4}\left(\frac{n^2\pi^2}{s^2}+M_2^2\omega_2^2r_2\right)\omega_1e_n^{(2)}\\ & -\left(\frac{2M_1^2M_2^2-\beta_1^2}{\beta_2^4}\right)\left(\frac{n^2\pi^2}{s^2}+M_2^2\omega_2^2r_1\right)\left[\frac{(1+\delta_{n,0})}{2}sR_n-\omega_1e_n^{(1)}\right]\\ & -\frac{2M_2^2}{\beta_2^4}\left(\frac{n^2\pi^2}{s^2}+\omega_2^2\right)\left[\frac{(1+\delta_{n,0})s}{2}Q_n-\omega_1iA_0(c_n^{(2)}-c_n^{(1)})\right],\end{aligned}$$

where

$$r_1 = \frac{M_1^2+1-(\beta_1^4/M_1^2)(\mu-1)/(\mu+1)}{2M_1^2M_2^2-\beta_1^2}, \quad r_2 = \frac{M_1^2+1}{2M_1^2M_2^2-M_1^2\beta_2^2}, \quad c_n^{(j)} \equiv \frac{1-\exp\{i(\sigma+n\pi)\}}{n^2\pi^2/s^2-M_j^2\omega_j^2}$$

and

$$e_n^{(j)} \equiv iA_0\frac{2(n^2\pi^2/s^2)c_n^{(j)}-i\omega_js^{\dagger}\exp\{i(\sigma+n\pi)\}}{n^2\pi^2/s^2-M_j^2\omega_j^2}+\omega_j(H_0-A_0d_0)c_n^{(j)}, \quad j=1,2.$$

Appendix G

In this appendix we use the solutions (3.21) and (3.27) to obtain an expression for the pressure distributions on the portion of the lower $n = 0$ blade surface lying between $x = 1-2s^\dagger$ and $x = 1-s^\dagger$. It follows from the periodicity condition (3.1) that the pressure in this region can be calculated from the pressure on the portion of the lower surface of the $n = 1$ blade that lies between $x = 1-s^\dagger$ and $x = 1$. We can again use the residue theorem to evaluate the integrals but here the integrands must each be divided into two terms and the contours must be closed in the lower half-plane for one of these and the upper half-plane for the other. Applying (3.1) to the results of these evaluations then yields

$$P_2^{(1)}(x,0-) \equiv \left(i\omega_2 - \frac{\partial}{\partial x}\right)\Phi_2^{(1)}(x,0-) = \sum_{n=0}^{\infty}\left\{\frac{\exp(i\eta_n^- \tilde{x}_2)}{\exp\{i(\sigma-\eta_n^- s^\dagger + n\pi)\}-1}\sum_{m=0}^{\infty} B_m K_{m,n}\right.$$
$$+ B_n\left[\frac{\exp(i\eta_n^+ x)}{\exp\{-i(\eta_n^+ s^\dagger - \sigma + n\pi)\}-1} + \frac{\exp\{i(\eta_n^+ - \sigma)\}}{2}\right.$$
$$\times(\exp\{-i(\sigma+n\pi)\} - \exp(-i\eta_n^+ s^\dagger))$$
$$\left.\left.\times\sum_{m=-\infty}^{\infty}\mathscr{K}_m^-(\lambda_n^{(2)})\exp\{-i(\alpha_m^- + M_2 k_2)(x-1+2s^\dagger)\}\right]\right\}$$
$$\text{for}\quad 1-2s^\dagger < x < 1-s^\dagger \qquad \text{(G 1)}$$

and

$$P_2^{(2)}(x,0-) = \left(i\omega_2 - \frac{\partial}{\partial x}\right)\Phi_2^{(2)}$$
$$= e^{-i\sigma}\sum_{n=0}^{\infty}\mathscr{K}_m^+(M_2 k_2)\exp\{-i(\alpha_m^- + M_2 k_2)(\tilde{x}_2 + s^\dagger)\}\left(D_-^{(2)} + \frac{i\omega_1 A_0}{\alpha_m^- + M_2 k_2}\right)$$
$$+\sum_{n=0}^{\infty}\frac{H_n \exp(i\eta_n^- \tilde{x}_2)}{[\exp\{i(\sigma-\eta_n^- s^\dagger + n\pi)\}-1]} - \omega_1\{2iA_0 + \omega_2[H_0 + A_0(x-d_0)]\}$$
$$\times\frac{\cot(M_2\omega_2 s)}{M_2\omega_2}$$
$$-i\omega_1 A_0\omega_2\frac{\partial}{\partial\omega_2}\left(\frac{\cot(M_2\omega_2 s)}{M_2\omega_2}\right)\quad\text{for}\quad 1-2s^\dagger < x < 1-s^\dagger, \qquad \text{(G 2)}$$

where

$$\mathscr{K}_m^{\pm}(\alpha) \equiv \frac{\kappa_2^{\pm}(-\alpha)(d_2^\dagger\Gamma_m^{(2)} - \alpha_m^- s^\dagger)}{\kappa_2^-(\alpha_m^-)d_2^\dagger(s^\dagger\Gamma_m^{(2)} - \alpha_m^- d_2^\dagger)[\sin(\alpha_m^- s^\dagger - d_2^\dagger\Gamma_m^{(2)})](\alpha_m^- + \alpha)}$$

and $\Gamma_m^{(2)}$, $d_2^\dagger$ and $\alpha_m^\pm$ are given by (E 2)–(E 4).

REFERENCES

Brix, C. W. & Platzer, M. F. 1974 Theoretical investigation of supersonic flow past oscillating cascades with subsonic leading edge locus. *A.I.A.A. 12th Aerospace Sci. Meeting*, paper 74-14.

Carlson, J. F. & Heins, A. E. 1947 Reflection of an electromagnetic plane wave by an infinite set of plates. *Quart. Appl. Math.* **4**, 313.

Coupry, G. & Piazzoli, G. 1958 Étude du flottement en régime transonique (study of flow at transonic speeds). *Recherche Aeronaut.* no. 63.

CROCCO, L. 1954 One-dimensional treatment of steady gas dynamics. In *High-Speed Aerodynamics and Jet Propulsion*, vol. III (ed. H. W. Emmons), pp. 64–350. Princeton University Press.

ECKHAUS, W. 1959 Two-dimensional transonic unsteady flow with shock waves. *Office Sci. Res. Tech. Note* no. 59–491.

FUNG, Y. C. 1955 *An Introduction to the Theory of Aeroelasticity*, pp. 166–168. Wiley.

GOLDSTEIN, M. E. 1975*a* Cascade with subsonic leading-edge locus. *A.I.A.A. J.* **13**, 1117.

GOLDSTEIN, M. E. 1975*b* On the kernel function for the unsteady supersonic cascade with subsonic leading edge locus. *N.A.S.A. Tech. Memo.* TMX-71673.

GOLDSTEIN, M. E. 1976 *Aeroacoustics*. McGraw-Hill.

KAJI, S. & OKAZAKI, T. 1970 Generation of sound by rotor–stator interaction. *J. Sound Vib.* **13**, 281.

KUROSAKA, M. 1974 On the unsteady supersonic cascade with a subsonic leading edge – an exact first-order theory. Part 2. *J. Engng Power* **96**, 23.

LANE, F. 1956 System mode shapes in the flutter of compressor blade rows. *J. Aero. Sci.* **23**, 54.

LANE, F. & FRIEDMAN, M. 1958 Theoretical investigation of subsonic oscillatory blade-row aerodynamics. *N.A.C.A. Tech. Rep.* no. 4136.

MANI, R. & HORVAY, G. 1970 Sound transmission through blade power. *J. Sound Vib.* **12**, 59.

MILLER, G. R. & BAILEY, E. E. 1971 Static-pressure contours in the blade passage at the tip of several high Mach number rotors. *N.A.S.A. Tech. Memo.* no. X-2170.

MOORE, F. K. 1954 Unsteady oblique interaction of a shock wave with a plane disturbance. *N.A.C.A. Rep.* no. 1165.

NAGASHIMA, T. & WHITEHEAD, D. S. 1974 Aerodynamic forces and moments for vibrating supersonic cascade blades. *Univ. Camb. Engng Dept. Rep.* CUED/A-Turbo/TR 59.

NOBLE, B. 1958 *Methods Based on the Wiener–Hopf Technique*. Pergamon.

SHAPIRO, A. H. 1953 *The Dynamics and Thermodynamics of Compressible Flows*, vol. 1. New York: Ronald Press.

VERDON, J. M. 1973 The unsteady aerodynamics of a finite supersonic cascade with subsonic axial flow. *J. Appl. Mech.* **40**, 667.

VERDON, J. & MCCUNE, J. 1975 The unsteady supersonic cascade in subsonic axial flow. *A.I.A.A. 13th Aerospace Sci. Meeting*, paper 75-22.